THE UNIVERSITY OF ALBERTA

JUMP RESONANCE IN A CLASS OF NONLINEAR CONTROL SYSTEMS

by

© Wilfred Chok Chung Ko

A THESIS

SUBMITTED TO THE FACULTY OF GRADUATE STUDIES

IN PARTIAL FULFILMENT OF THE REQUIREMENTS FOR THE DEGREE

OF MASTER OF SCIENCE

DEPARTMENT OF ELECTRICAL ENGINEERING

EDMONTON, ALBERTA

OCTOBER, 1967

UNIVERSITY OF ALBERTA

FACULTY OF GRADUATE STUDIES

The undersigned certify that they have read, and recommend to the Faculty of Graduate Studies for acceptance, a thesis entitled Jump Resonance in a Class of Nonlinear Control Systems submitted by Wilfred C.C. Ko in partial fulfilment of the requirements for the degree of Master of Science.

ABSTRACT

The outputs of certain nonlinear control systems are known to exhibit jumps in their values when the amplitude or frequency of the sinusoidal input signals is varied. A semi-graphical method is presented to determine this jump. This method is applicable to the class of control systems where there is a single-valued, piecewise continuous nonlinearity in the feedback loop. The application of this method to a system with a limiter is discussed. The predicted values are verified by analog computer studies. Agreement between calculated and experimental results for third order systems is very good; for second order systems the agreement is fair. Use of proportional derivative compensation as a method of eliminating jumps in the output is also examined both analytically and experimentally.

ACKNOWLEDGEMENTS

The author wishes to express his appreciation of the encouragement and guidance received during the course of this work from Dr. V. Gourishankar.

The work was carried out at the Department of Electrical Engineering of the University of Alberta. The financial assistance provided by this Department and the National Research Council is gratefully acknowledged. Thanks are due to the staff and graduate students of the Department for their advice and assistance.

TABLE OF CONTENTS

Table of Contents (cont'd) Page

NOMENCLATURE

Symbol	Meaning	Symbol First Appears on Page
a	maximum input level to limiter before saturation is reached	18
A_i	amplitude of input signal $r(t)$	7
A_o	amplitude of output signal $c(t)$	7
B	saturation level of limiter	18
B_o	amplitude of output of nonlinear element $c_1(t)$	7
$c(t)$	output of system	3
$c_1(t)$	output of nonlinear element	7
CR	distance from origin of X-Y plane to centre of constant A_o circles	10
DF	describing function	2
DIDF	dual input describing function	3
$e(t)$	error signal	3
EN	envelope of constant A_o circles	13
$G(s)$	transfer function of a linear plant	3
$G'(s)$	transfer function of equivalent linear plant with linear compensation	52
K	constant forward gain in G	28
K_t	constant factor in output derivative feedback loop	52
m	slope of a straight line	14
M	magnification factor	7

Nomenclature (cont'd)

Symbol	Meaning	Symbol First Appears on Page
$N(A_o)$	describing function of nonlinear element	3
$N'(A_o)$	first derivative of N with respect to A_o	9
$N''(A_o)$	second derivative of N with respect to A_o	12
$r(t)$	input signal	3
RA	radius of constant A_o circles	10
S	slope of limiter	18
$X(\omega)$	real part of $G(\omega)$	8
$Y(\omega)$	imaginary part of $G(\omega)$	8
$\emptyset$	phase shift at output of system	7
subscript j	means at "jump resonance"	13

LIST OF FIGURES, GRAPHS AND TABLES

List of Figures, Graphs and Tables (cont'd)

CHAPTER ONE
INTRODUCTION

1.1 General

It is well known that the steady state output of nonlinear feedback systems when subjected to a sinusoidal input often exhibits one or more of the following phenomena: limit cycles, jump resonance and sub-harmonics. Most of these characteristics, which are associated uniquely with nonlinear systems, have been extensively investigated by, among many others, Hayashi(1)*, Ogata(2), Lewis(3), West, Douce and Livesley(4), Prince, Jr.(5) and Levinson(6). Many of these investigators have shown particular interest in the study of jump resonance.

1.2 Method of Analysis

Jump resonance is a phenomenon in which a sinusoidal input signal with a fixed frequency and amplitude may give rise to outputs of more than one frequency or with multivalued amplitudes.

In his paper, Levinson(6) considers sinusoidal steady state and uses a semigraphical technique to obtain the multivalued output and the jump resonance conditions in a tachometer-stabilized system which consists of a linear plant and a nonlinear element. In essence, he equates

---

Footnote: * The numbers in parenthesis refer to the articles listed in the bibliography.

1.2 Method of Analysis (cont'd)

the equivalent gain of the nonlinear element, expressed as a function of the error signal to an expression involving the parameters of the linear plant, the input amplitude and the error. The latter expression represents a family of curves with ω, the radian frequency of the input signal, as a parameter. By plotting both sides of the above equation separately on the same graph, and in terms of the error, he is able to determine the jumps in the amplitude of the output by noting the point(s) of intersection of the family of curves and the curves representing the equivalent gain of the nonlinear element.

Ogata's analytic approach[2] is more interesting. His prediction of jump phenomenon and subharmonic oscillations is based on a method in which the generally accepted Describing Function (D.F.) gives way to the Laplace Transform technique. The Laplace Transform approach has a significant advantage over the describing function method in that the assumption of a sinusoidal input signal to the nonlinear element which is necessary in the describing function method is no longer required, and it is therefore applicable to all types of periodic waveforms such as square wave, triangular wave, etc. However, the usefulness of this method depends upon whether or not the waveform of the output of the nonlinear element in question is known. For instance, Ogata assumes that the waveform of the output of the nonlinear element is trapezoidal. The approximation of the output waveform by a trapezoid may or may not be a good one in all cases. In view of this basic limitation, and the fact that the

1.2 Method of Analysis (cont'd)

method involves rather lengthy and complicated mathematical manipulations, even in the case of a second order system, its acceptance over the describing function in solving nonlinear control problems has been limited.

Another method, similar to Levinson's, is that due to West et.al.[4]. In this method the authors employ the concept of Dual Input Describing Function (D.I.D.F.) and determine by a semigraphical procedure the occurrence of jump phenomena. The region of jump is indicated in the complex plane. The details of this approach will not be discussed here due to the limitations of space. It should be mentioned, however, that this method is even more complicated than Levinson's method.

More recently Hatanaka[7] has proposed a technique for determining the frequency response of closed-loop feedback systems. By this method, the conditions governing jump resonance can be obtained analytically. Like almost all other investigators, Hatanaka has treated the class of feedback systems in Fig. 1.1 in which the nonlinear element is in the forward path and in series with the linear part of the system. The closed loop system has unity feedback. Hatanaka assumes that the nonlinear element is single-valued and its Describing Function is independent of frequency of the input.

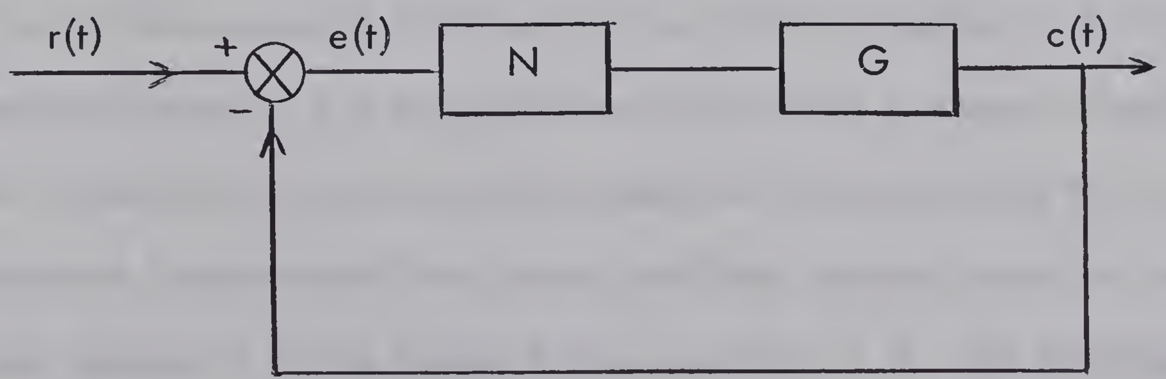

Fig. 1.1 System with nonlinearity in forward loop

1.2 Method of Analysis (cont'd)

Some of Hatanaka's main results are summarized in Appendix A. We observe that E, the amplitude of the error signal e(t) is the independent variable in all the expressions. Hatanaka's approach is not directly applicable to the class of nonlinear systems in which the nonlinear element is located in the feedback path (Fig. 1.2) for two reasons. Firstly, the independent variable now becomes A_o, the output amplitude. Secondly, the phase shift between r(t) and $c_1(t)$ must be taken into account.

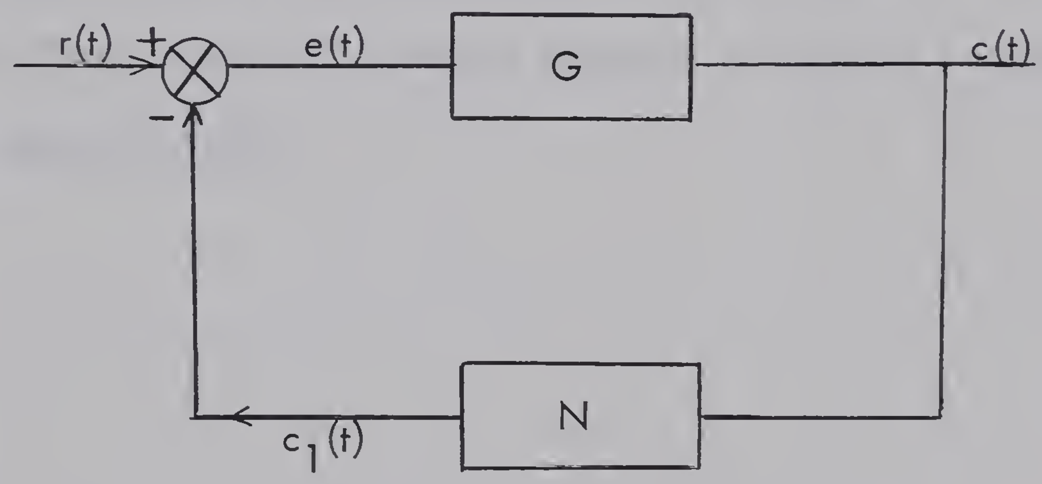

Fig. 1.2 System with nonlinearity in feedback loop

1.3 Objective of This Thesis

Since Hatanaka's method is completely analytical, one is likely to overestimate its usefulness. However, practical implementation of this procedure is difficult in view of the complexity of the expressions derived. It is the objective of this thesis to present a method that is partly analytical and partly graphical for determining the jump resonance frequencies of the class of nonlinear systems where the nonlinear element is in the feedback loop as in Fig. 1.2. The investigation

1.3 Objective of This Thesis (cont'd)

will be confined to systems in which nonlinearity is single-valued and whose describing function is independent of the frequency of inputs. The nonlinearity will be represented by its Describing Function since we will be considering sinusoidal inputs to the system. Furthermore, Describing Functions of commonly encountered nonlinearities have been derived and are available in the literature [8,9]. It is assumed, however, that the linear plant G acts as a low pass filter and tends to attenuate the higher order harmonics in the output of the nonlinear element. This assumption is necessary (and hopefully realized) to make the Describing Function approach valid.

CHAPTER TWO

DERIVATION OF CONDITIONS FOR JUMP RESONANCE

2.1 Input-Output Relationship

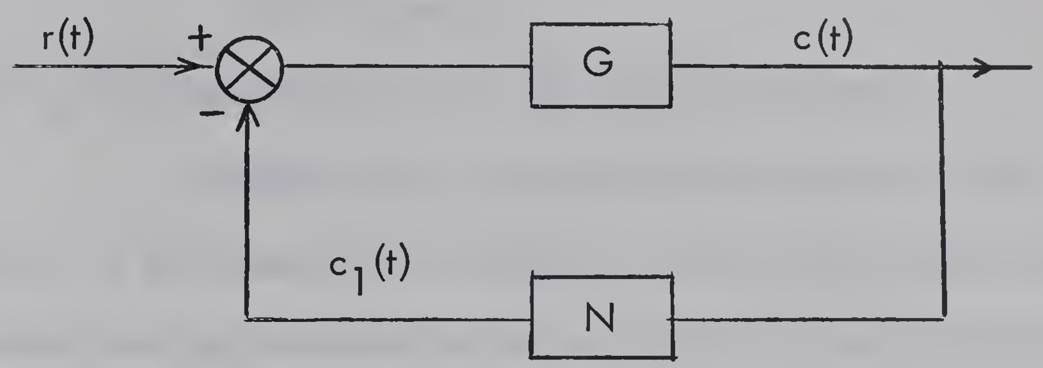

Fig. 2.1 System with nonlinearity in feedback loop

As mentioned in the previous chapter, the jump resonance conditions will be derived for a system in which the nonlinear element is in the feedback path. The configuration shown in Fig. 1.2 is redrawn in Fig. 2.1 for easy reference. G(s) is the transfer function of the linear portion of the plant; N is the describing function of the nonlinear element. We will restrict N to satisfy the following conditions:

(a) N is single-valued and frequency independent. This excludes energy storage elements which have hysteresis.

(b) N is dependent only on the signal amplitude A_o at its input.

(c) N is twice-differentiable with respect to A_o. Conditions (a) and (b) are easily met by many commonly-encountered nonlinear elements. Since most nonlinearities in practice are piecewise continuous, or at least their shapes can be represented by piecewise continuous functions, requirement (c) poses no real difficulty in most cases.

2.1 Input-Output Relationship (cont'd)

We will determine the steady state response c(t) of such a system when subjected to a single sinusoidal input r(t). Let

$$r(t) = A_i \sin \omega t \tag{2.01}$$

where A_i is the amplitude and ω is the angular frequency.

In steady state, the output of the system will be periodic. If the linear plant is assumed to be a good low pass filter, this output can be considered to be sinusoidal and can be represented by its fundamental component or first harmonic. Let this component be

$$c(t) = A_o \sin(\omega t + \emptyset) \tag{2.02}$$

where A_o is the amplitude and $\emptyset$ the phase shift. This c(t) is the input to the nonlinear element.

Under conditions (a) and (b), the nonlinear element is represented by its describing function $N(A_o)$. If $c_1(t)$ is the fundamental component of the output of the nonlinear element, and

$$c_1(t) = B_o \sin(\omega t + \emptyset_1) \tag{2.03}$$

then

$$N(A_o) = \frac{B_o}{A_o} \tag{2.04}$$

In the frequency domain, the output-input amplitude ratio of the system is given by

$$M = \left| \frac{G(\omega)}{1 + G(\omega)\, N(A_o)} \right| = \frac{A_o}{A_i} \tag{2.05}$$

2.1 Input-Output Relationship (cont'd)

Let $G(\omega)$ be separated into its real and imaginary parts, that is

$$G(\omega) = X(\omega) + j\,Y(\omega) \tag{2.06}$$

Substituting equation (2.06) into (2.05), we get

$$A_i = \frac{\sqrt{(1 + NX)^2 + (NY)^2}}{\sqrt{X^2 + Y^2}}\, A_o \tag{2.07}$$

Here $N(A_o)$, $X(\omega)$, $Y(\omega)$, are written as N. X, Y, respectively for brevity.

2.2 Conditions for Jump Resonance

With the signal frequency held constant, we now determine the input amplitude when output displays an abrupt jump; that is, we want the points at which

$$\left.\frac{\partial A_o}{\partial A_i}\right|_{\omega = \text{const}} = \infty \tag{2.08a}$$

or equivalently,

$$\left.\frac{\partial A_i}{\partial A_o}\right|_{\omega = \text{const}} = 0 \tag{2.08b}$$

2.2 Conditions for Jump Resonance (cont'd)

These conditions are illustrated graphically in Fig. 2.2.

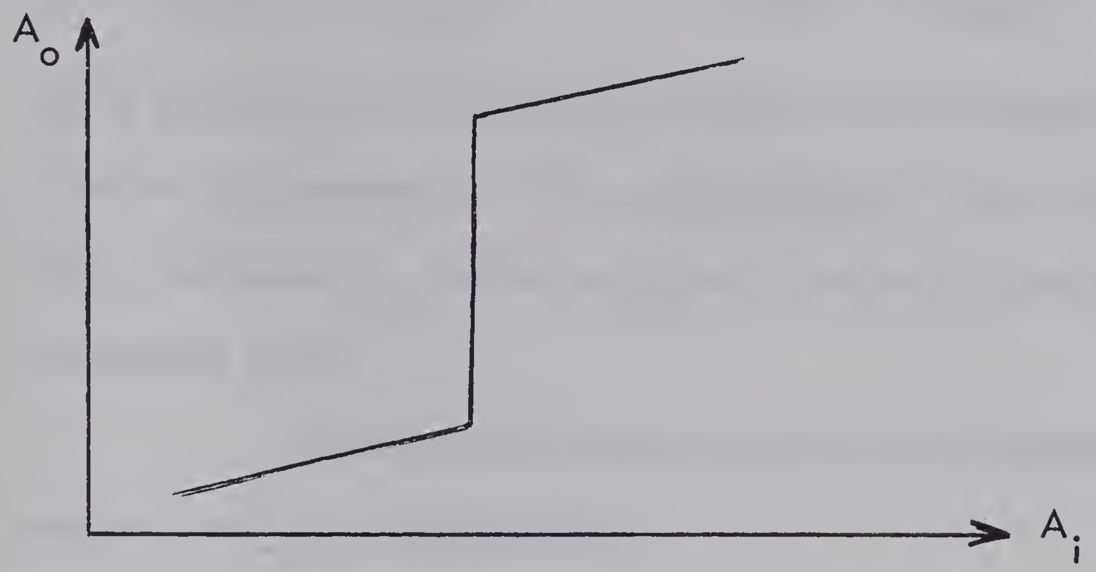

Fig. 2.2 Input-output curve with a jump

Using equation 2.07, we find that

$$\left.\frac{\partial A_i}{\partial A_o}\right|_{\omega = \text{const}} = \frac{1}{\sqrt{X^2 + Y^2}} \left\{ \sqrt{(1 + NX)^2 + (NY)^2} \right.$$

$$\left. + A_o \left[(1 + NX)^2 + (NY)^2\right]^{-1/2} \bullet \left[(1 + NX)X \frac{dN}{dA_o} + (NY)Y \frac{dN}{dA_o}\right] \right\} \quad (2.09)$$

By setting this expression equal to zero, we get

$$(1 + NX)^2 + (NY)^2 + A_o (X + NX^2 + NY^2) \frac{dN}{dA_o} = 0 \qquad (2.10)$$

or

$$X^2 (N^2 + NN'A_o) + Y^2 (N^2 + NN'A_o) + X(2N + N'A_o) + 1 = 0 \qquad (2.11)$$

where $\dfrac{dN}{dA_o} = N'$

Equation (2.11) gives the condition for jump resonance. This result can be further rearranged into a more convenient form:

2.2 Conditions for Jump Resonance (cont'd)

$$\left[X + \frac{2N + N'A_o}{2(N^2 + NN'A_o)}\right]^2 + Y^2 = \left[\frac{N'A_o}{2(N^2 + NN'A_o)}\right]^2 \qquad (2.12)$$

This is the equation of a family of circles in the X-Y plane with N and A_o as parameters. But, as noted earlier, N is a function of A_o, and hence A_o can be considered to be the only parameter in equation 2.12.

The centres of these circles are on the negative real axis and their coordinates are

$$\left[\frac{2N + N'A_o}{2\,(N^2 + NN'A_o)}\ ,\ 0\right] \qquad (2.13)$$

The distance from origin to the centre is

$$CR = \frac{2N + N'A_o}{2\,(N^2 + NN'A_o)} \qquad (2.14)$$

The radius of each circle is

$$RA = \left|\frac{N'A}{2\,(N^2 + NN'A_o)}\right| \qquad (2.15)$$

As A_o takes on different values, the radius and the relative position of the centres change. Fig. 2.3 shows one possible situation for three values of A_o.

2.2 Conditions for Jump Resonance (cont'd)

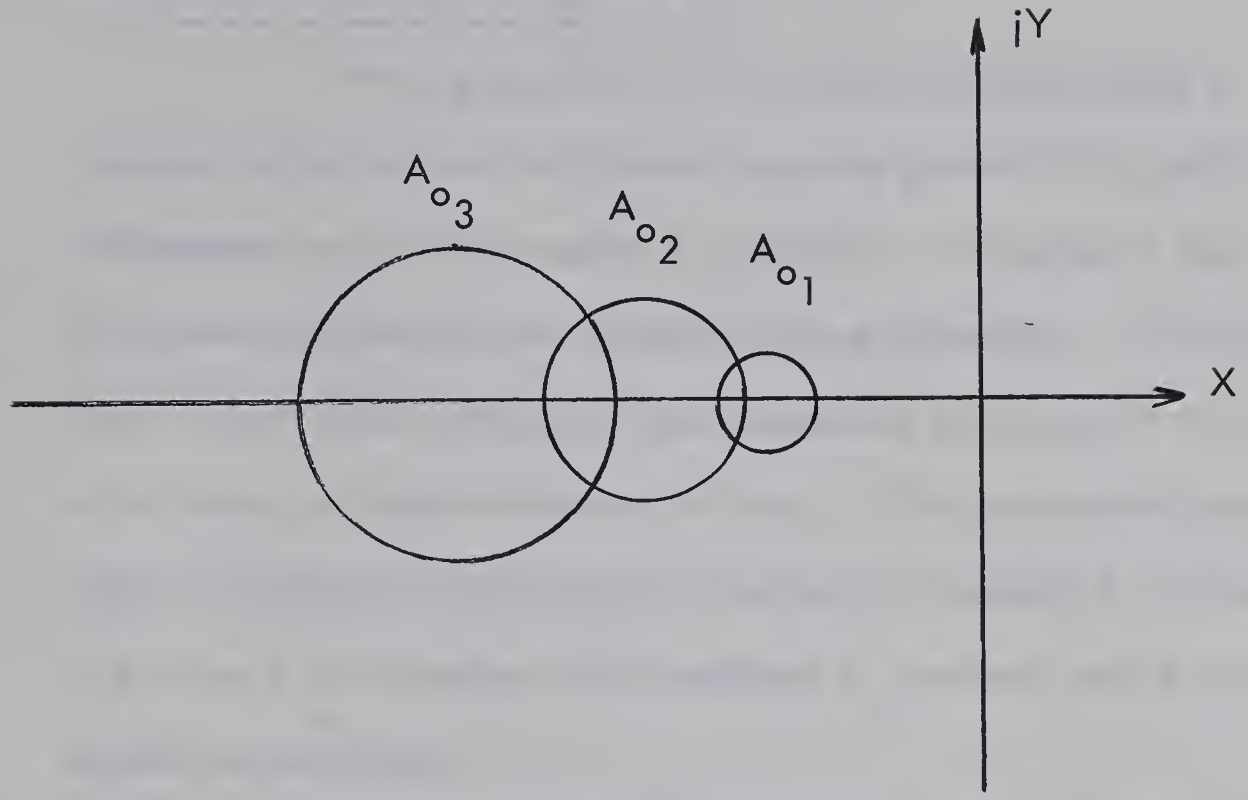

Fig. 2.3 Circles on G plane

Jump resonance conditions are indicated if the plot of G (ω) in the X-Y plane, and the family of circles in Fig. 2.3, intersect. This is shown in Fig. 2.4.

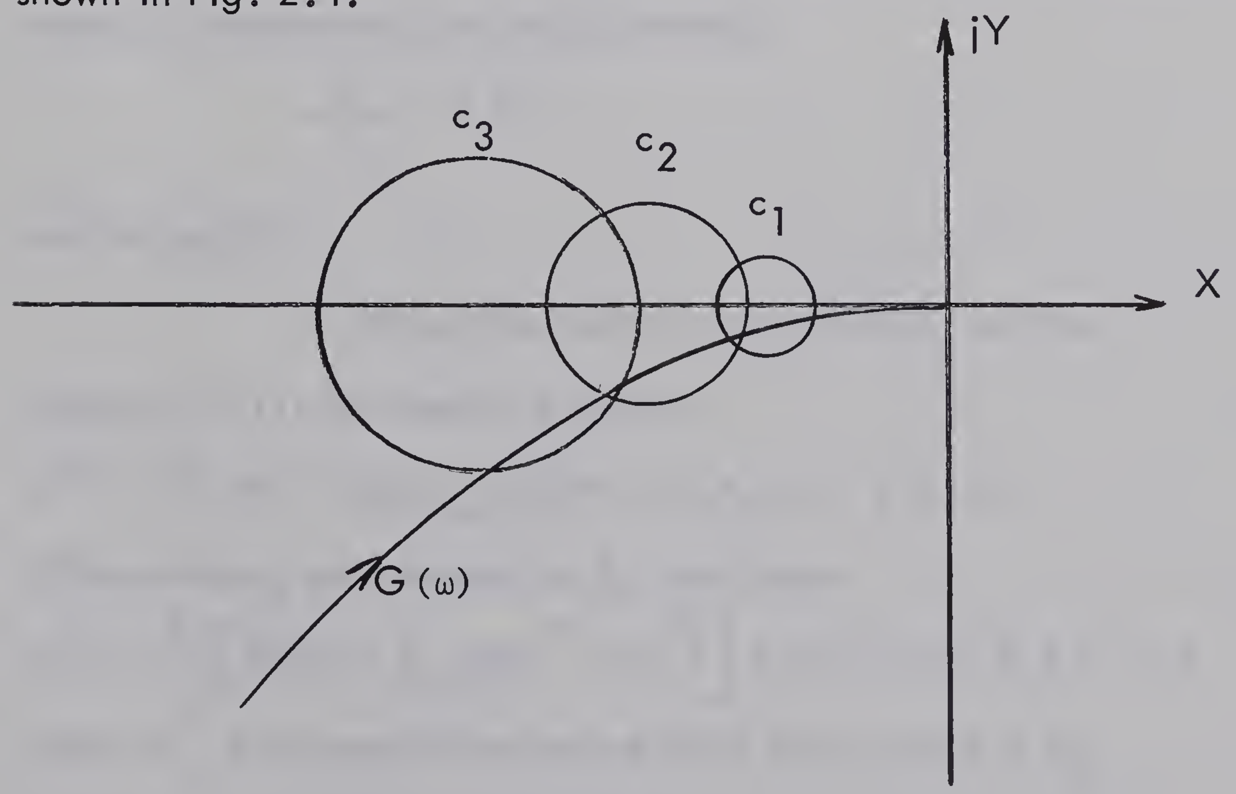

Fig. 2.4 Occurrence of jump resonance

2.3 Envelope of the Constant A_o Contours

For a given G (ω), it is easily seen that there is a region in the complex X-Y plane where the plot of G (ω) will not intersect any of the constant A_o contours. The region in the X-Y plane can therefore be divided into two subregions. If G (ω) lies in one of these subregions, jump resonance occurs and if it lies in the other, no jump resonance will occur. The curve which separates these two regions is that which just touches the constant A_o circles. This curve is the envelope of the constant A_o contours, and it can be determined as follows:

It is well known [10] that the envelope of a family of curves given by

$$f(x, y, c) = 0 \tag{2.16}$$

where x, y are variables and c is a parameter is obtained by eliminating c in equation 2.16 and by setting

$$\frac{\partial f}{\partial c} = 0 \tag{2.17}$$

and solving for c.

In the problem under consideration, we have (equation 2.11) the family of circles

$$(X^2 + Y^2)\ (N^2 + NN'A_o) + (2N + N'A_o)\,X + 1 = 0 \tag{2.11}$$

Differentiating with respect to A_o, we obtain

$$(X^2 + Y^2)\left[3NN' + A_o\,(NN'' + N'^2)\right] + (3N' + N''A_o)\,X = 0 \tag{2.18}$$

where N'' is the second derivative of N with respect to A_o.

2.3 Envelope of the Constant A_o Contours (cont'd)

For the nonlinear elements under consideration, N, N' and N'' are all functions of A_o, and therefore, A_o can be eliminated in the equations (2.11) and (2.18). However, in practice these computations may be very cumbersome and a digital computer may be used to advantage. This will be done in this thesis also.

2.4 Input Amplitude at Jump Resonance Point

In this section we will use the envelope obtained earlier and determine frequency and amplitude of the input signal at which jump resonance occurs. Figure 2.5 shows a case where the envelope EN and $G(\omega)$ are shown intersecting each other at point P.

Let the co-ordinates of P be (X_i, Y_i) and let the associated frequency be ω_i. It must be remembered that ω is a parameter along the $G(\omega)$ curve.

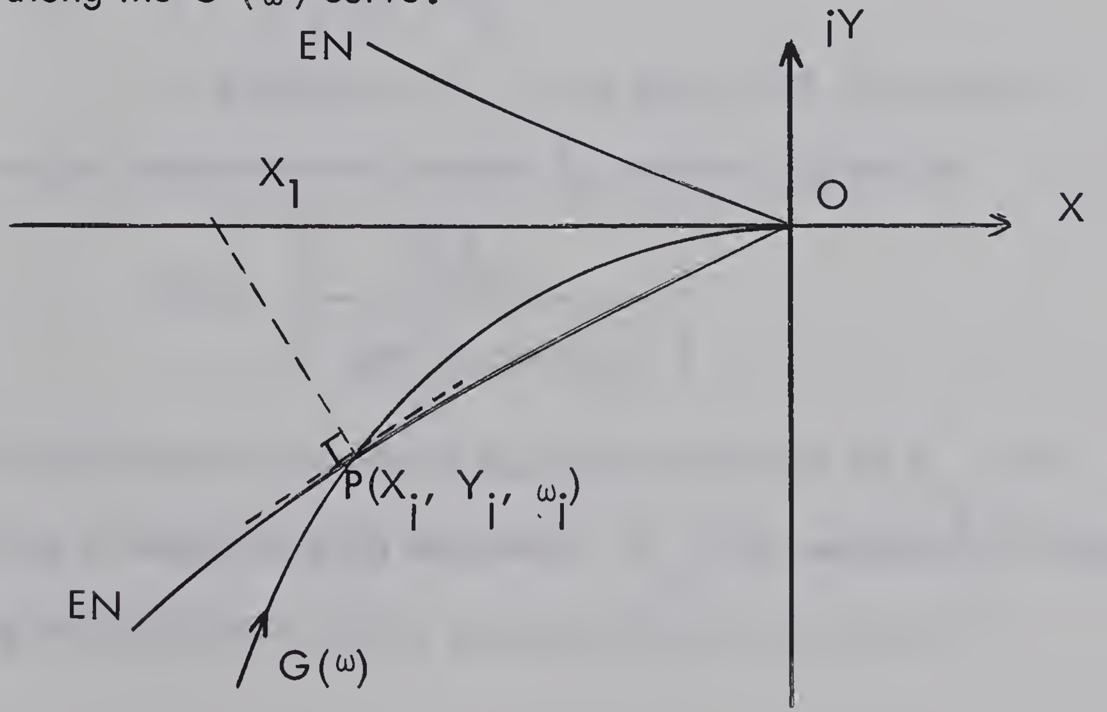

Fig. 2.5 Construction for the location of the centre of a constant A_o circle

2.4 Input Amplitude at Jump Resonance Point (cont'd)

The envelope EN can be considered to represent a function of X and Y. A tangent to EN has a slope m where

$$m = \frac{\partial Y}{\partial X} \tag{2.19}$$

At the point P,

$$m_i = \left(\frac{\partial Y}{\partial X}\right)_i \tag{2.20}$$

It is shown in Appendix B that the equation of a straight line passing through P and perpendicular to the tangent at P is

$$Y = -\frac{1}{m_i} X + Y_i + \frac{1}{m_i} X_i \tag{2.21}$$

This straight line cuts the X axis at the point X_1 where

$$X_1 = m_i Y_i + X_i \tag{2.22}$$

Let the distance from P to X_1 be L, then

$$L = \sqrt{(X_1 - X_i)^2 + Y_i^2} = \sqrt{(m_i Y_i)^2 + Y_i^2}$$

or

$$L = |Y_i| \sqrt{1 + m_i^2} \tag{2.23}$$

In equation 2.15, it was shown that the radius of circle which represents the constant A_o contour is given by

$$RA = \left| \frac{N' A_o}{2(N^2 + NN' A_o)} \right| \tag{2.24}$$

Equations 2.23 and 2.24 can be equated and solved for A_{o_i}, the amplitude of output at jump resonance. A_{i_i}, the amplitude of input at jump resonance can now be computed from equation 2.07.

2.4 Input Amplitude at Jump Resonance Point (cont'd)

$$A_{i_i} = \frac{\sqrt{(1 + NX_i)^2 + (NY_i)^2}}{\sqrt{X_i^2 + Y_i^2}} A_{o_i} \qquad (2.25)$$

2.5 Graphical Approach

The analytical method, developed in the previous Section, is exact. However, the computations required in some of the steps are very tedious. For example, it is quite difficult to obtain an analytic equation for the envelope expressed explicitly in terms of X and Y. Even for a relatively simple nonlinear element such as the limiter, the elimination of A_o from equations (2.11) and (2.17) is difficult because N, N' and N'' are nonlinear functions of A_o. In the case of a nonlinear element represented by a more complicated describing function, the analysis will be prohibitively involved. Fortunately, a semi-graphical method can be used. The result obtained by this method will probably be less accurate than that obtained by the analytical method, but the graphical method has the advantage of being simple and easy to apply.

We will now outline this semi-graphical method by which the input amplitude at jump resonance can be found quite readily. The method consists of five broad steps. Figure 2.6 will be used to describe these steps.

2.5 Graphical Approach (cont'd)

(1) Both EN and G (ω) are plotted (generally this will involve the use of a digital computer) on the same graph, and their points of intersection P and Q designated by $(X_{j1}, Y_{j1}, \omega_{j1})$ and $(X_{j2}, Y_{j2}, \omega_{j2})$ respectively are found. That part of G (ω) lying in the region between P and Q and bounded by the envelope is the region of jump resonance. Operation in this region will cause a discontinuous jump at the output. The frequencies ω_{j1} and ω_{j2} are respectively the lower and upper limits of the frequency of the input signal between which jump resonance occur.

(2) Within the region of jump resonance, let D be an arbitrary point where jump resonance occurs for certain conditions. Draw a tangent to G (ω) at this point.

(3) The straight line perpendicular to the tangent is constructed to cut the X axis at point X_c. This then is the centre of the constant A_o circles which just touches G (ω) at the point D. We will refer to this as the critical circle.

2.5 Graphical Approach (cont'd)

(4) The distance from the origin to X_c is now known. This can be substituted into equation 2.14 and the value of A_{o_i} can be obtained by solving the following equation:

$$CR\Big|_{X_c} = \frac{2N + N' A_{o_i}}{2\,(N^2 + NN' A_{o_i})} \qquad (2.26)$$

where N and N' are expressed as function of A_{o_i}.

(5) Once A_{o_i} is known, the corresponding input amplitude can be calculated from equation 2.25.

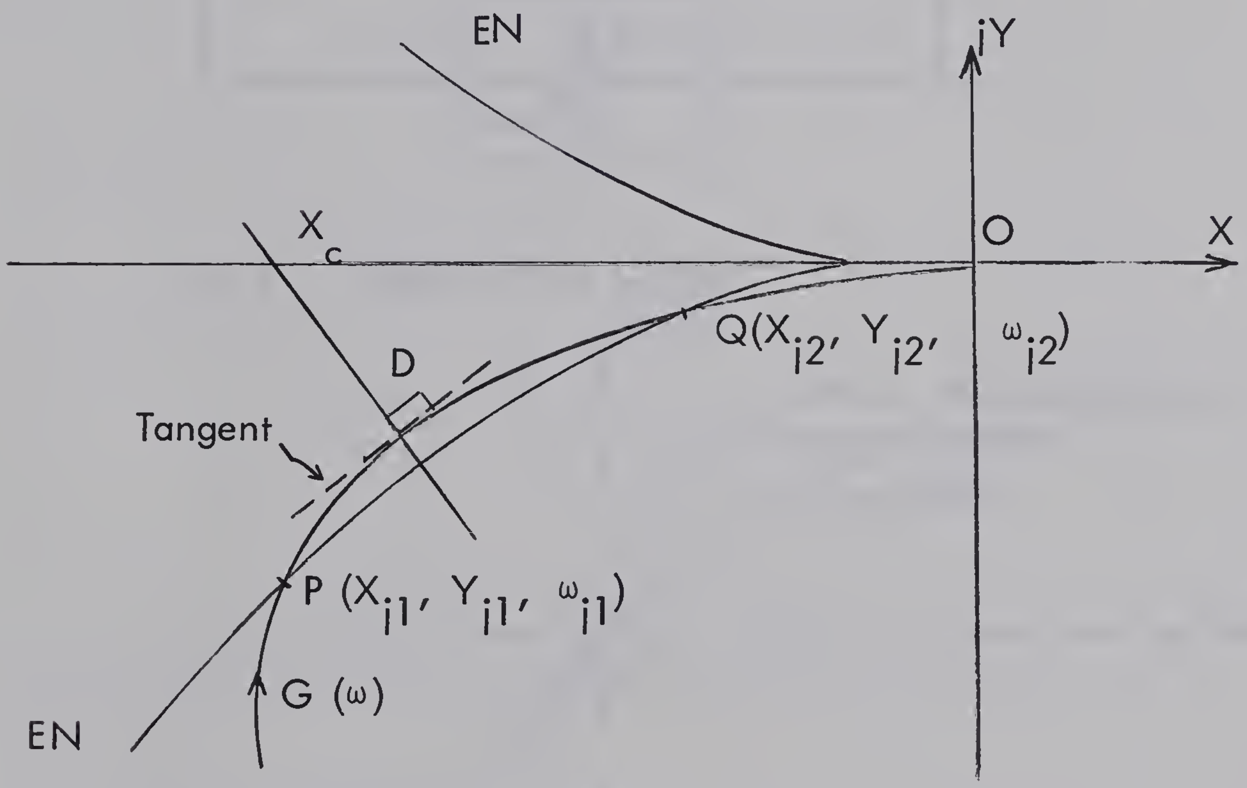

Fig. 2.6 Graphical technique

CHAPTER THREE

JUMP RESONANCE PHENOMENON IN A SYSTEM WITH A LIMITER

3.1 Introduction

In this chapter, the semigraphical method described in the preceding chapter will be applied to a feedback control system (Figure 3.1) in which the nonlinear element is a limiter.

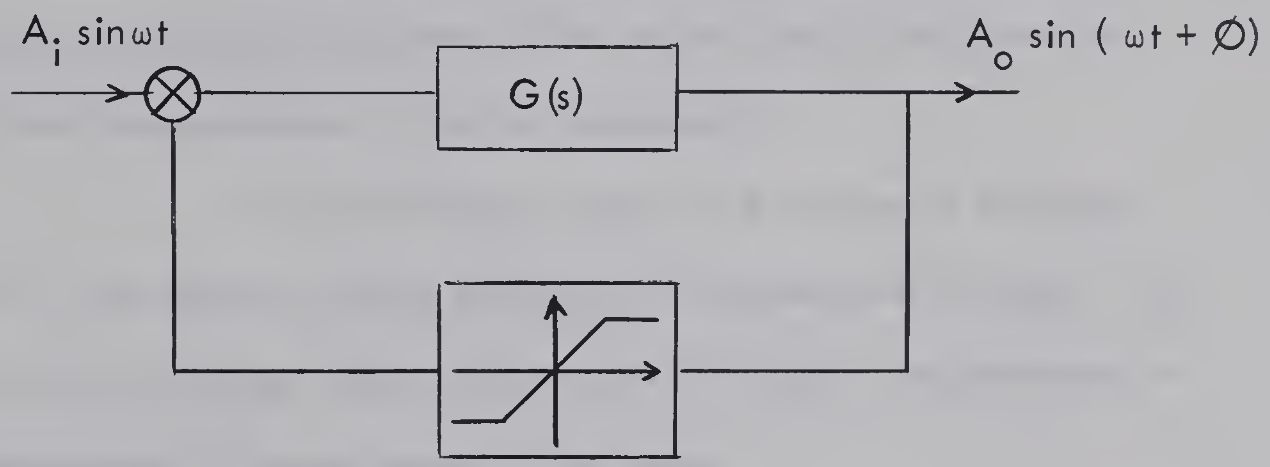

Fig. 3.1 System with a Limiter

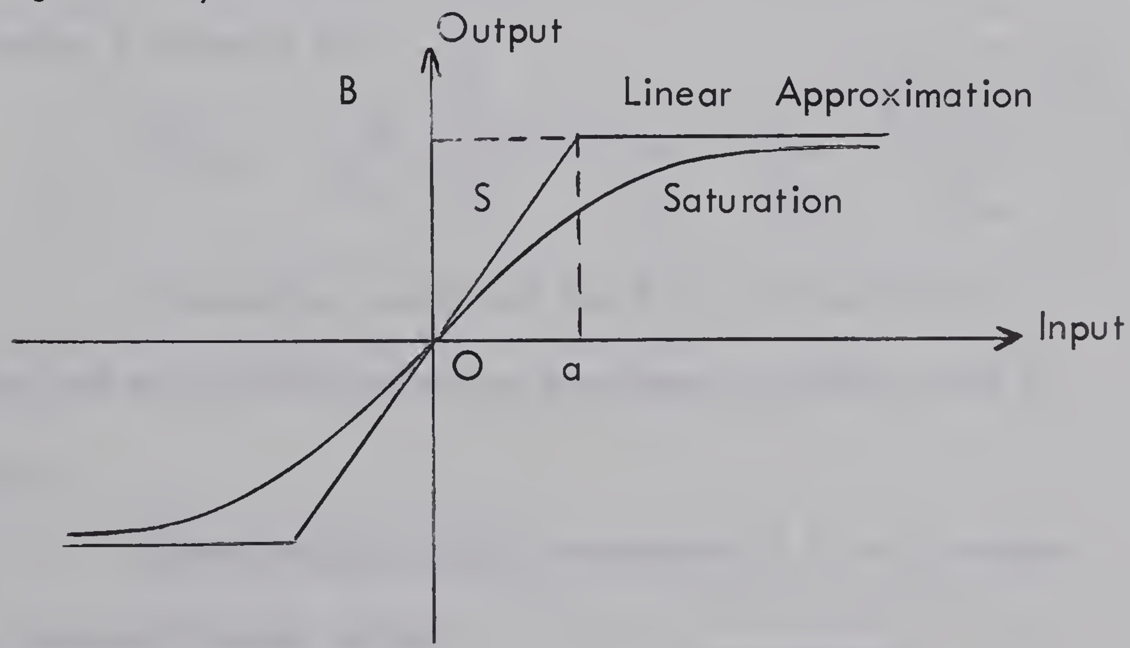

Fig. 3.2 Transfer characteristics of a saturation type nonlinearity and its linear approximation

3.1 <u>Introduction (cont'd)</u>

The limiter has been chosen because it is very commonly encountered in practice. Amplifiers are, for example, linear only over a limited range of operation; a two-phase motor has a maximum shaft speed; and a hydraulic transmission used as a motor device has a maximum output speed.

Figure 3.2 shows the transfer characteristic of a saturation type nonlinearity. The limiter can be considered as a linear approximation of such a nonlinearity.

For small signal inputs in the range oa in Figure 3.2, the device is linear and output is proportional to input. For sufficiently large inputs, output remains constant and becomes independent of the magnitude of the input.

In Appendix C, the describing function (D.F.) of the limiter is shown to be

$$N(A_o) = \frac{2B}{\pi a}\left[\sin^{-1}\left(\frac{a}{A_o}\right) + \frac{a}{A_o}\,\frac{\sqrt{A_o^2 - a^2}}{A_o}\right] \tag{3.01}$$

It should be noted that the D.F. is frequency independent and as such the procedure developed in Chapter Two is applicable.

Differentiating $N(A_o)$ in equation 3.01 with respect to A_o successively twice, we get

$$N'(A_o) = -\frac{4B}{\pi a}\left(\frac{a}{A_o^2}\right)\sqrt{1 - \left(\frac{a}{A_o}\right)^2} \tag{3.02}$$

3.1 Introduction (cont'd)

or

$$N'(A_o) \cdot A_o = -\frac{4B}{\pi a}\left(\frac{a}{A_o}\right)\sqrt{1-\left(\frac{a}{A_o}\right)^2} \qquad (3.03)$$

and

$$N''(A_o) = -\frac{4B}{\pi}\;\frac{\frac{a^2}{A_o} - 2A_o\left[1-\left(\frac{a}{A_o}\right)^2\right]}{A_o^4\sqrt{1-\left(\frac{a}{A_o}\right)^2}} \qquad (3.04)$$

An examination of the above expressions reveals that $N'(A_o)$ and $N''(A_o)$ become imaginary when

$$\frac{a}{A_o} > 1 \qquad (3.05)$$

It will be recalled that equations (2.11) and (2.18) which determine the condition for jump resonance contain N' and N''. Consequently, for jump resonance to take place, the inequality 3.05 must be satisfied. This is in accordance with the physical situation at hand. When $A_o < a$, the system is operating in a linear region with a variable gain S in the feedback loop. In this linear range of operation, no jumps are possible. Unless otherwise stated, inequality (3.05) is assumed to hold throughout this thesis.

3.2 Constant A_o Circles in the X-Y Plane

In this section we will examine the location of the constant A_o circles in the X-Y plane for the system shown in Figure 3.1. We will also examine the envelope of these circles.

3.2 Constant A_o Circles in the X-Y Plane (cont'd)

From Chapter Two, we have

$$CR = \frac{2N + N'A_o}{2N\,(N + N'A_o)} \qquad [2.14]$$

where CR is the distance of the centre of the constant A_o circles from the origin in the X-Y plane. Substituting equations (3.10) and (3.03) into (2.14) for N and $N'A_o$, we get

$$CR = \frac{\sin^{-1}\left(\frac{a}{A_o}\right)}{\frac{2B}{\pi a}\left\{\left[\sin^{-1}\left(\frac{a}{A_o}\right)\right]^2 - \left(\frac{a}{A_o}\right)^2\left[1 - \left(\frac{a}{A_o}\right)^2\right]\right\}} \qquad (3.06)$$

Expanding the denominator in a power series, we get

$$CR = \frac{\sin^{-1}\left(\frac{a}{A_o}\right)}{\frac{2B}{\pi a}\left\{\left[\frac{a}{A_o} + \frac{1}{6}\left(\frac{a}{A_o}\right)^3 + \dots\right]^2 - \left(\frac{a}{A_o}\right)^2 + \left(\frac{a}{A_o}\right)^4\right\}} \qquad (3.07)$$

Clearly, the right hand side of equation (3.07) is always positive. This indicates CR, the centre of constant A_o is confined to the left half of the X-Y plane.

Similarly, the radius of the constant A_o circles is obtained from equation (2.15) as

$$RA = \frac{\left(\frac{a}{A_o}\right)\sqrt{1 - \left(\frac{a}{A_o}\right)^2}}{\frac{2B}{\pi a}\left\{\left[\sin^{-1}\left(\frac{a}{A_o}\right)\right]^2 - \left(\frac{a}{A_o}\right)^2\left[1 - \left(\frac{a}{A_o}\right)^2\right]\right\}} \qquad (3.08)$$

3.2 Constant A_o Circles in the X-Y Plane (cont'd)

We then determine the difference between CR and RA,

$$CR - RA = \frac{\sin^{-1}\left(\frac{a}{A_o}\right) - \left(\frac{a}{A_o}\right)\sqrt{1 - \left(\frac{a}{A_o}\right)^2}}{\frac{2B}{\pi a}\left\{\left[\sin^{-1}\left(\frac{a}{A_o}\right)\right]^2 - \left(\frac{a}{A_o}\right)^2\left[1 - \left(\frac{a}{A_o}\right)^2\right]\right\}} \tag{3.09}$$

This can be simplified into

$$CR - RA = \frac{1}{\frac{2B}{\pi a}\left[\sin^{-1}\left(\frac{a}{A_o}\right) + \left(\frac{a}{A_o}\right)\sqrt{1 - \left(\frac{a}{A_o}\right)^2}\right]} \tag{3.10}$$

Again, expanding the denominator in a power series, (4.10) becomes

$$CR - RA = \frac{1}{\frac{2B}{\pi a}\left[\frac{a}{A_o} + \frac{1}{6}\left(\frac{a}{A_o}\right)^3 + \ldots + \left(\frac{a}{A_o}\right) - \frac{1}{2}\left(\frac{a}{A_o}\right)^3 + \ldots\right]} \tag{3.11}$$

Since $\frac{a}{A_o} < 1$, we can retain only first and third order terms without much loss of accuracy:

$$CR - RA \approx \frac{1}{\frac{2B}{\pi a}\left[\frac{2a}{A_o} - \frac{1}{3}\left(\frac{a}{A_o}\right)^3\right]} \tag{3.12}$$

The right hand side is always positive, therefore

$$CR > RA$$

3.2 Constant A_o Circles in the X-Y Plane (cont'd)

This assures that all the circles will lie on the left half of the X-Y plane.

If $\frac{a}{A_o} \ll 1$, we can neglect the third order term also in equation (3.12) and we get

$$CR - RA \approx \frac{\pi A_o}{4B} = \frac{\pi}{4} \cdot \frac{a}{B} \cdot \frac{A_o}{a} > \frac{a}{B} \qquad (3.13)$$

Now consider the limiting case when $\frac{a}{A_o} \to 1$.

The circle diminishes in size and approaches a point since RA in equation (3.08) approaches zero. The difference between CR and RA, in the limit, can be obtained exactly from equation (3.10) by substituting $\frac{a}{A_o} = 1$. Thus,

$$CR - RA = \frac{a}{B} \qquad (3.14)$$

or

$$CR - RA = \frac{1}{S} \qquad (3.15)$$

since the slope $S = \frac{B}{a}$

It can be concluded that in the case of a system with the limiter as the nonlinear element as shown in Figure 3.1, all constant A_o circles are confined to the left of the limiting line

$$X = -\frac{a}{B} \qquad (3.16)$$

3.2 Constant A_o Circles in the X-Y Plane (cont'd)

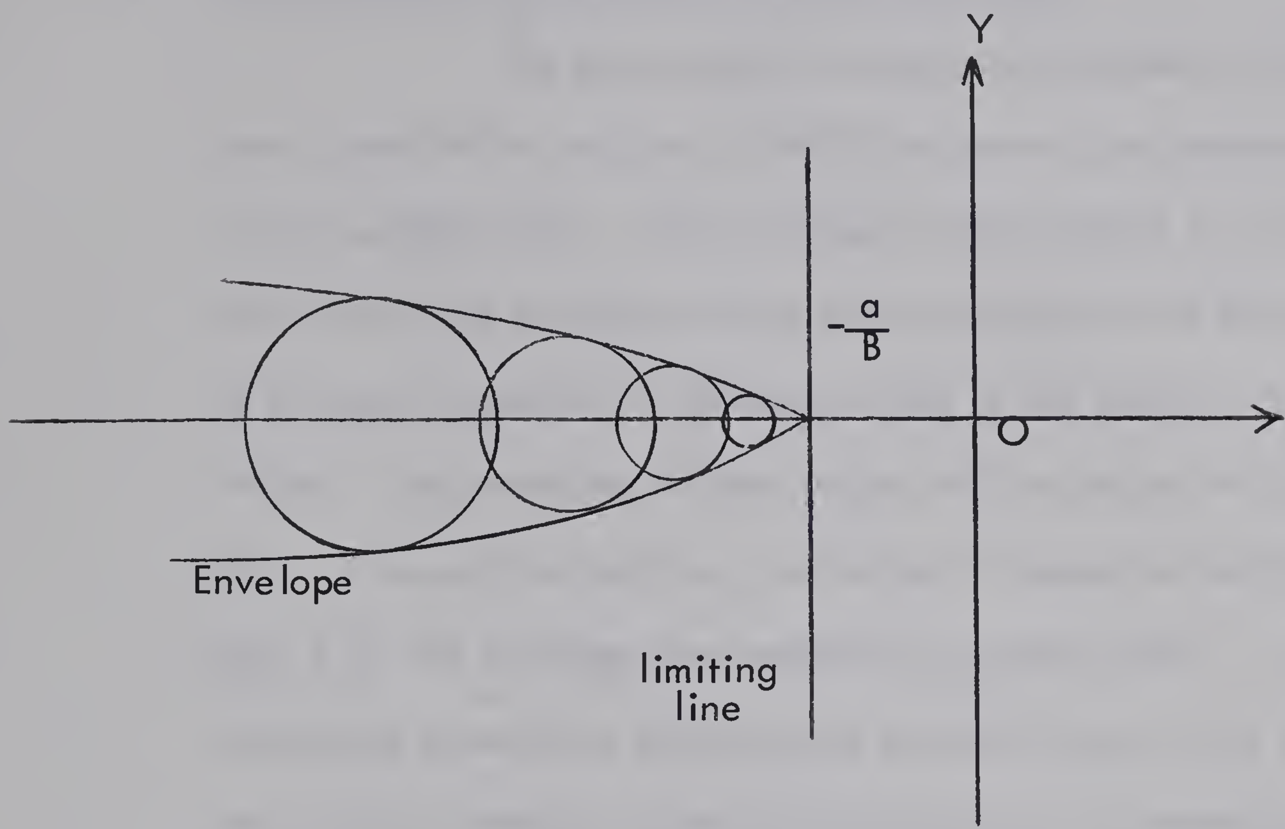

Fig. 3.3 Limiting line and constant A_o circles

The location of this limiting line on the X-Y plane, as shown in Figure 3.3, depends on the slope of the limiter. In the case of a limiter with a steep slope, the limiting line will be close to the origin. It is expected that intersection (if any) with the $G(\omega)$ locus will be at the high frequency portion of the $G(\omega)$ curve. On the other hand, in the case of a limiter with a small slope, the limiting line will be quite far away from the origin, and intersection of $G(\omega)$ and the envelope will probably be confined to the lower frequency portion of the $G(\omega)$ curve.

3.3 Determination of the Region of Jump Resonance

The semi-graphical approach described in Chapter Two is used in this section to find the region of jump resonance in the complex plane. The envelope of the constant A_o circles which forms the boundary of this region is plotted with the help of a digital computer for different values of the slopes of the limiter. The envelopes for four values of S are shown in Figure 3.4. It is worth noting that, for values of S equal to and less than 1/2, the envelopes are comparatively more linear. Further, the region bounded by the envelope becomes larger as the slope of the limiter increases, so that the possibility of its intersection with $G(\omega)$ also increases even though the forward gain K associated with $G(\omega)$ may be small. These and other aspects of jump resonance will be illustrated by means of examples in the sections that follow.

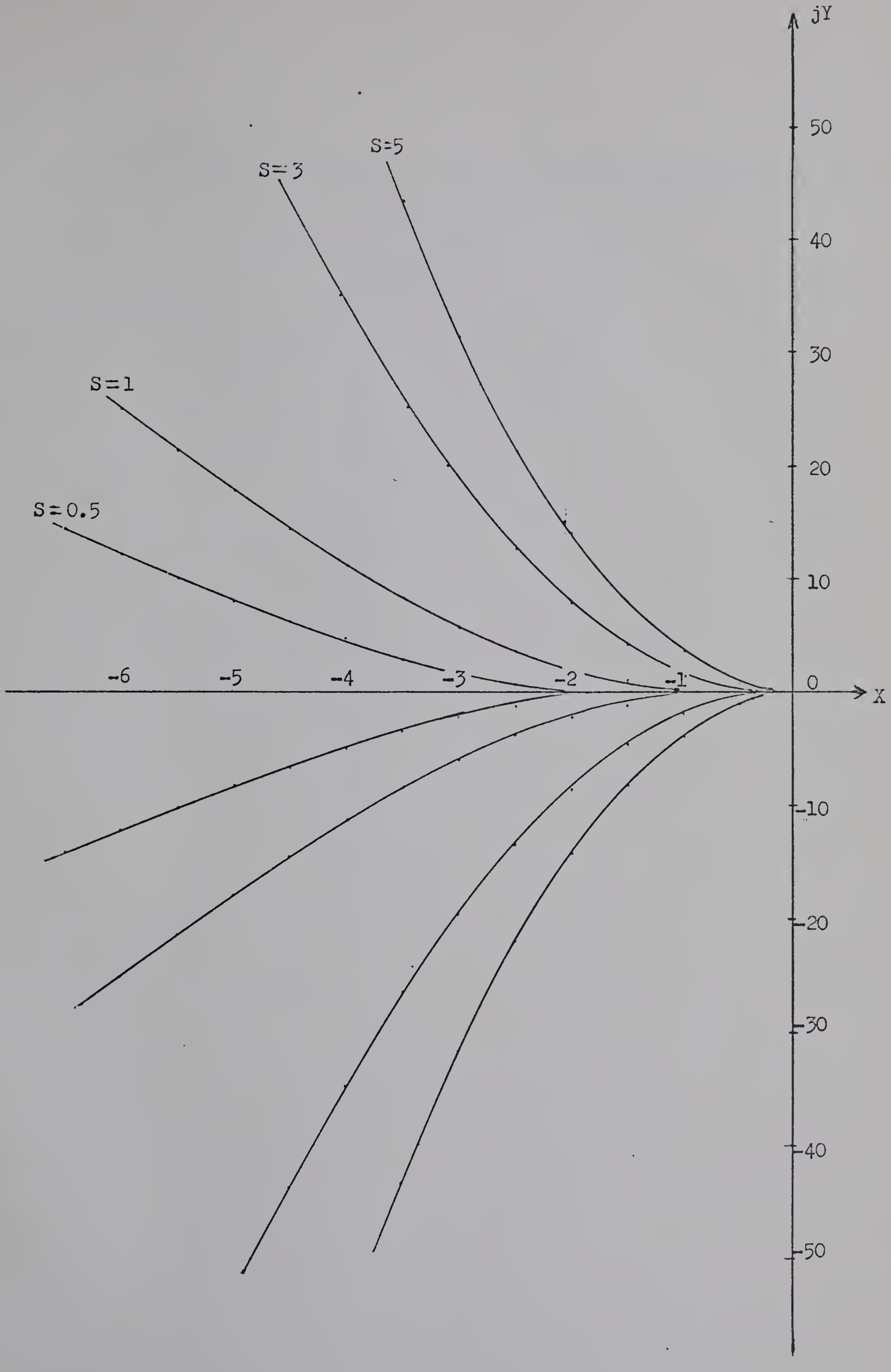

Fig. 3.4 Envelopes of Constant A_o Circles for Different Values of S

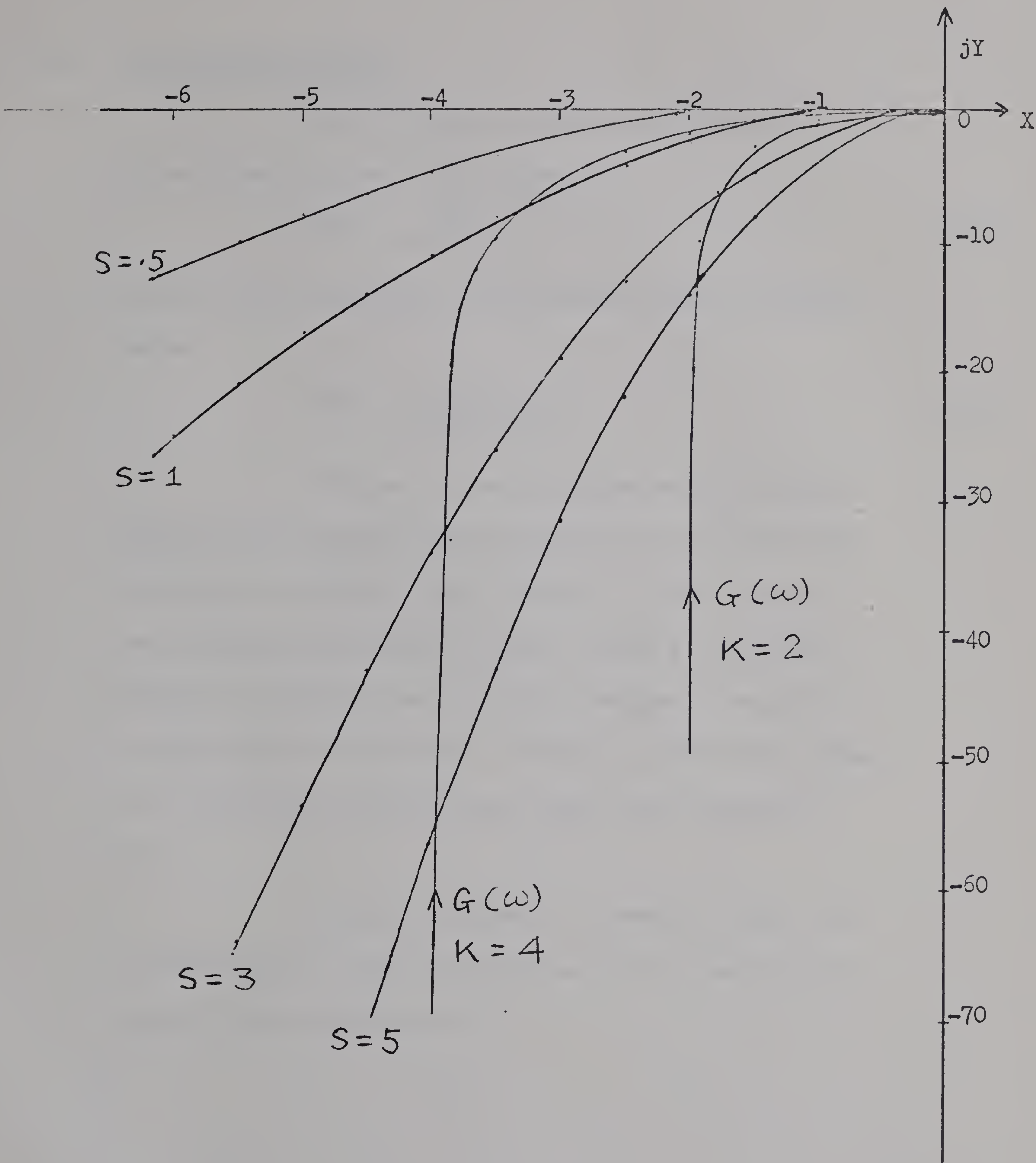

Fig. 3.5 Envelopes of Constant A_o Circles and G Loci

3.4 A Second Order System

We will choose a simple second order plant whose transfer function is G(s), where

$$G(s) = \frac{K}{s\,(s+1)} \tag{3.17}$$

where K is the constant gain and is assumed to take on different values.

$$G(\omega) = \frac{K}{j\omega\,(1 + j\omega)} \tag{3.18}$$

In Figure 3.5, we have drawn only the relevant portion of the envelopes together with two curves of $G(\omega)$ when K takes on two different values. When $K = 4$, $G(\omega)$ intersects the envelopes corresponding to slopes 1, 3 and 5 of the limiter. When $K = 2$, $G(\omega)$ intersects only two envelopes corresponding to slopes 3 and 5 of the limiter. Therefore, a limiter with a slope of 1 will not cause a discontinuous output at any frequency if $K = 2$.

A portion of Figure 3.5 is redrawn in Figure 3.6 for better clarity, and we shall make use of it to examine some aspect of jump resonance at $K = 2$.

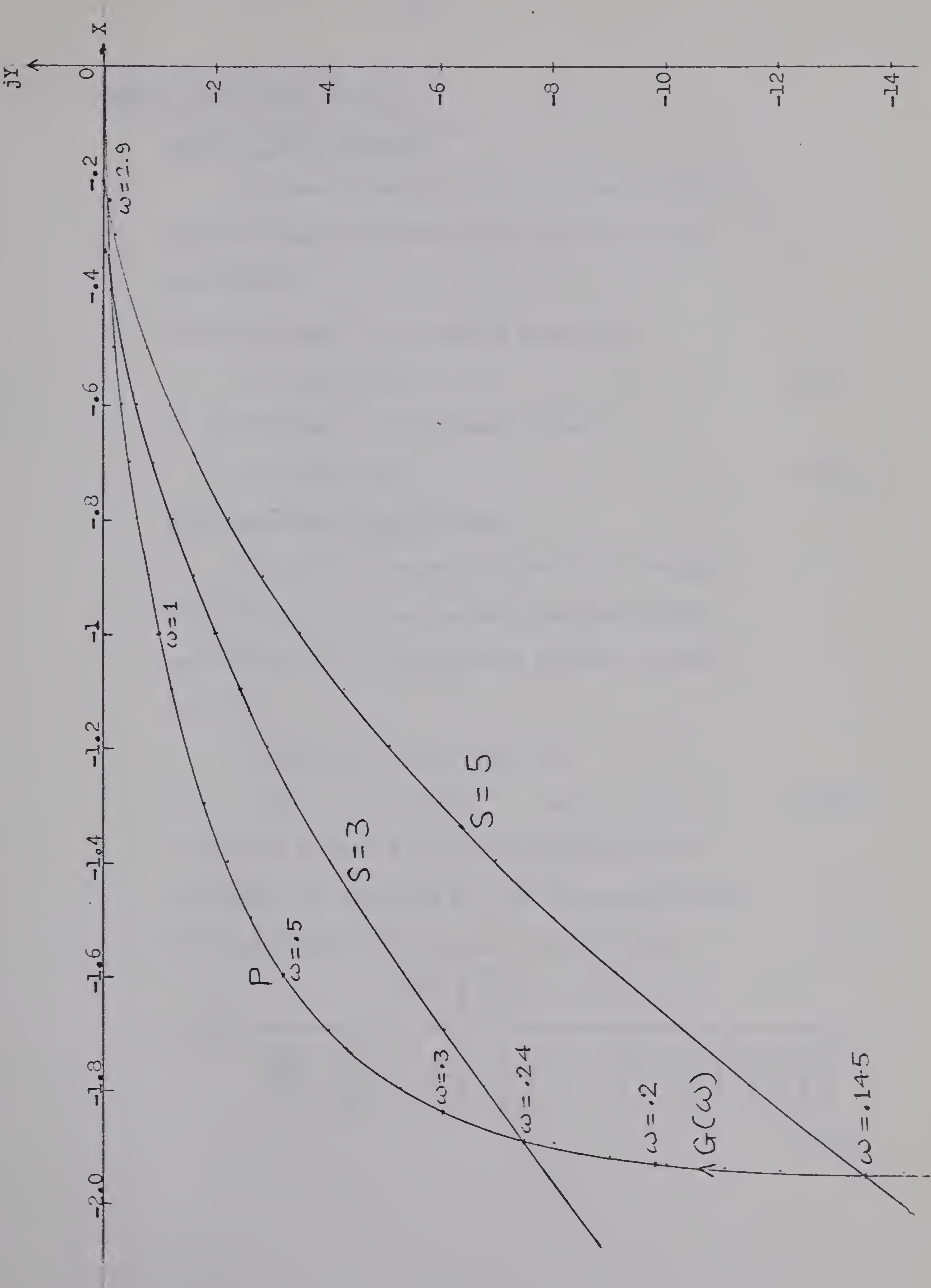

Fig. 3.6 Region of jump resonance for second order system. K = 2

3.4 A Second Order System (cont'd)

Region of jump resonance

By inspection of Figure 3.6, it is seen that the range of frequency at which jump resonance will occur is as follows:

For limiter slope = 5, the range of frequency is

$$0.15 \leq \omega_i \leq 2.9 \tag{3.19}$$

For limiter slope = 3, the frequency range is

$$0.24 \leq \omega_i \leq 2.2 \tag{3.20}$$

Input amplitude at jump resonance

We will pick one point on the $G(\omega)$ curve lying within the region of jump resonance and determine the input amplitude using the procedure outlined in section 2.5.

At the point P, (see Figure 3.6)

$$X_i = -1.6, \qquad Y_i = -3.2 \qquad \text{and } \omega_i = 0.5 \tag{3.21}$$

A tangent is drawn at P and the line perpendicular to this tangent cuts the X axis at -1.81. The absolute value 1.81 is substituted for CR in equation (3.07). Thus

$$1.81 = \frac{\sin^{-1}\left(\frac{a}{A_o}\right)}{\frac{2B}{\pi a}\left\{\left[\frac{a}{A_o} + \frac{1}{6}\left(\frac{a}{A_o}\right)^3 + \dots\right]^2 - \left(\frac{a}{A_o}\right)^2 + \left(\frac{a}{A_o}\right)^4\right\}} \tag{3.22}$$

3.4 A Second Order System (cont'd)

Input amplitude at jump resonance (cont'd)

As assumed previously, contribution from higher order terms is negligible, so that equation (3.22) can be simplified further as

$$1.81 = \frac{\frac{a}{A_o} + \frac{1}{6}\left(\frac{a}{A_o}\right)^3}{\frac{2B}{\pi a}\left[\frac{4}{3}\left(\frac{a}{A_o}\right)^4\right]} \tag{3.23}$$

or

$$1.81 = \frac{1 + \frac{1}{6} V^2}{\frac{8}{3\pi} \cdot \frac{B}{a} \cdot V^3} \tag{3.24}$$

where $V = \frac{a}{A_o}$ for convenience.

Consider the following cases:

Case 1 slope $\frac{B}{a} = 5$

Substituting for $\frac{B}{a}$ in equation (3.24), we get

$$7.68\, V^3 - 0.167\, V^2 = 1 \tag{3.25}$$

We are interested only in the real solution of this equation and it is easily found to be

$$V_i = 0.515 \tag{3.26}$$

Let $a = 1$, then, since $\frac{a}{A_{o_i}} = 0.515$,

$$A_{o_i} = 1.94 \tag{3.27}$$

3.4 A Second Order System (cont'd)

Input amplitude at jump resonance (cont'd)

From equation (3.01)

$$N = \frac{2B}{\pi a}\left[\sin^{-1} V + V\sqrt{1 - V^2}\right] \tag{3.28}$$

Substituting for $\frac{B}{a}$ and V_j in (3.28) we get

$$N = 3.04 \tag{3.29}$$

Now, the input amplitude can be found from equation (2.25) where

$$A_{i_j} = \frac{\sqrt{(1 + NX_j)^2 + (NY_j)^2}}{\sqrt{X_j^2 + Y_j^2}} \; A_{o_j} = 5.7 \tag{3.30}$$

Case 2 slope $\frac{B}{a} = 3$

In the same manner, we obtain the following results:

$$V = 0.478 = \frac{a}{A_o} \tag{3.31}$$

$$A_{o_j} = 2.09 \tag{3.32}$$

$$N = 1.72 \tag{3.33}$$

and

$$A_{i_j} = 3.32 \tag{3.34}$$

3.5 A Third Order System

Consider the third order plant with transfer function G(s) where

$$G(s) = \frac{K}{s(s+1)(s+2)}, \qquad K = 2 \tag{3.35}$$

3.5 A Third Order System (cont'd)

As before, the envelopes and $G(\omega)$ are plotted on the same graph paper as shown in Figure 3.7. In this case, the higher frequency portion of $G(\omega)$ lies in the upper half plane so that the upper points of intersection with envelopes are also in this upper half plane.

Frequency range for jump resonance

For limiter slope = 5 $$0.125 \leq \omega_i \leq 1.7 \tag{3.36}$$

For limiter slope = 3 $$0.23 \leq \omega_i \leq 1.4 \tag{3.37}$$

The point we choose for consideration is Q where

$$X_i = -1.25, \quad Y_i = -1.92 \quad \omega_i = 0.4 \tag{3.38}$$

From this we find CR = 1.42 (3.39)

Omitting details, we find the following results:

Case 3

slope $\frac{B}{a} = 5$

$V_i = 0.56$

$A_{o_i} = 1.78$

$N = 3.25$

and $$A_{i_i} = 5.3 \tag{3.40}$$

Case 4

slope $\frac{B}{a} = 3$

$V_i = 0.67$

$A_{o_i} = 1.49$

$N = 2.21$

$$A_{i_i} = 2.96 \tag{3.41}$$

3.5 A Third Order System (cont'd)

The accuracy of the values as obtained in sections 3.4 and 3.5 will be verified when we compare them with experimental values which we will present in the next chapter.

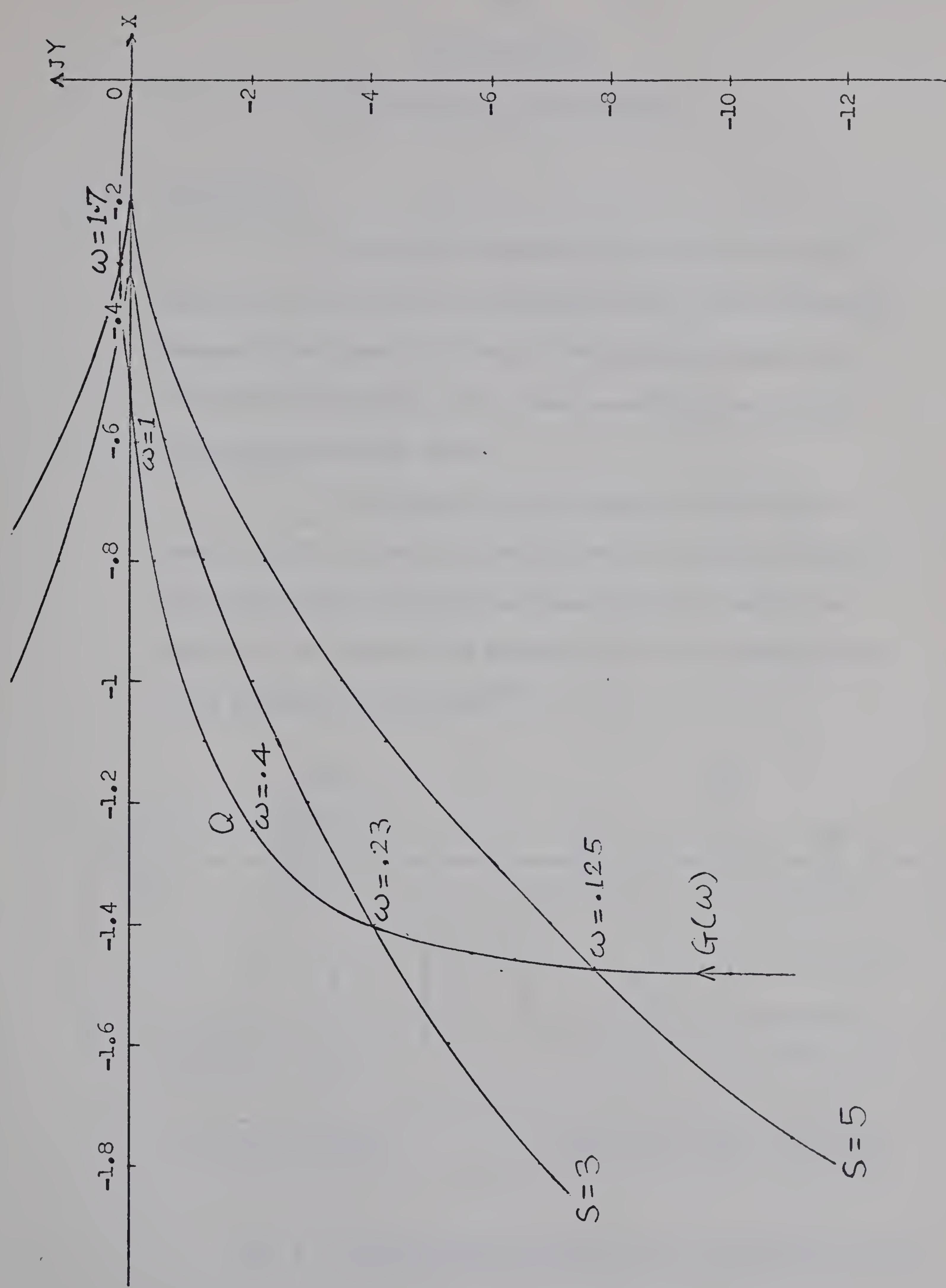

Fig. 3.7 Region of jump resonance for third order systems. K = 2

CHAPTER FOUR

EXPERIMENTAL VERIFICATIONS

4.1 Introduction

This chapter is devoted to a discussion of the experimental results which were obtained by using a PACE 231R analog computer. The systems considered in the preceding chapter were simulated on the computer with a view to verifying the accuracy of the predictions made earlier.

The schematic computer diagrams for the system shown in Fig. 3.1 when G is a second order linear plant and when G is a third order linear plant are shown in Fig. 4.1 and 4.2 respectively. The details of the simulation will not be discussed here as the procedure is well known[12].

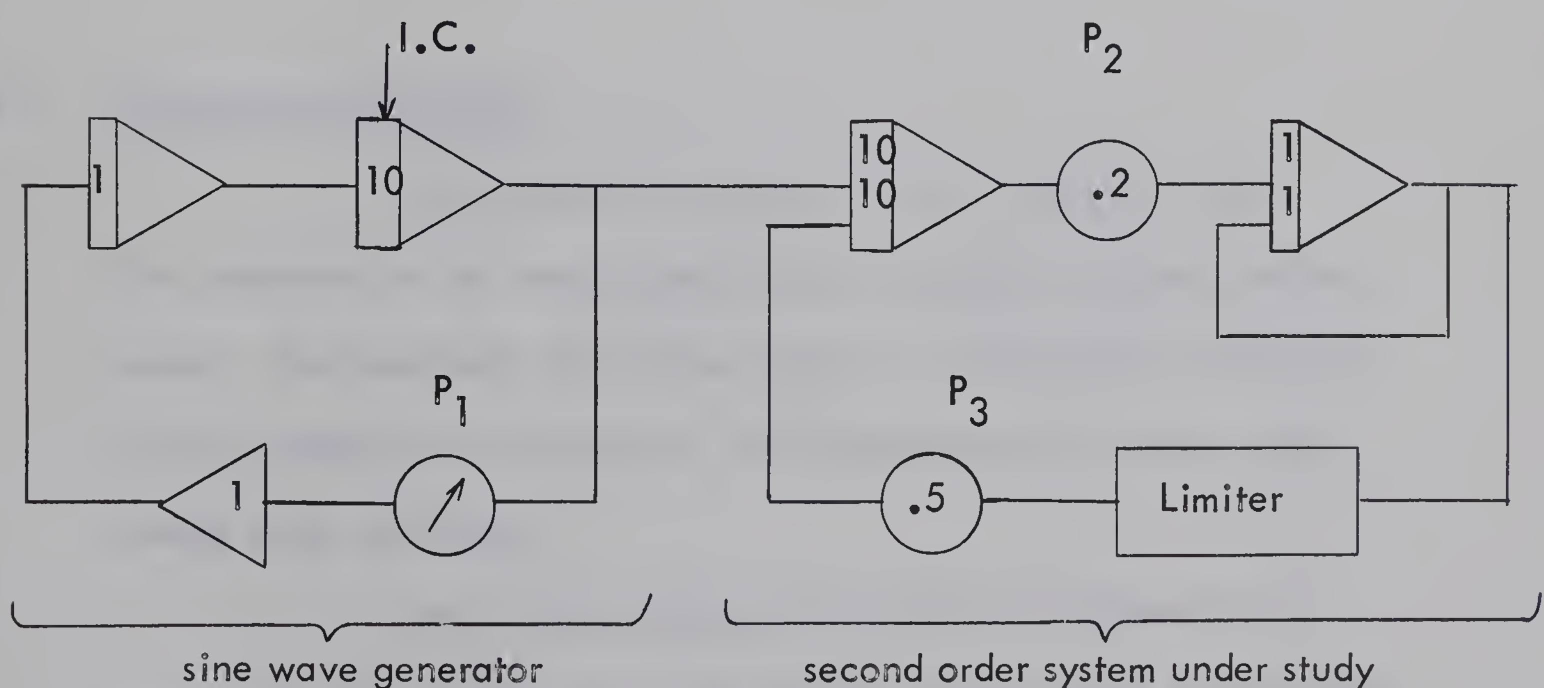

Fig. 4.1 Analog computer simulation for a second order system

4.1 Introduction (cont'd)

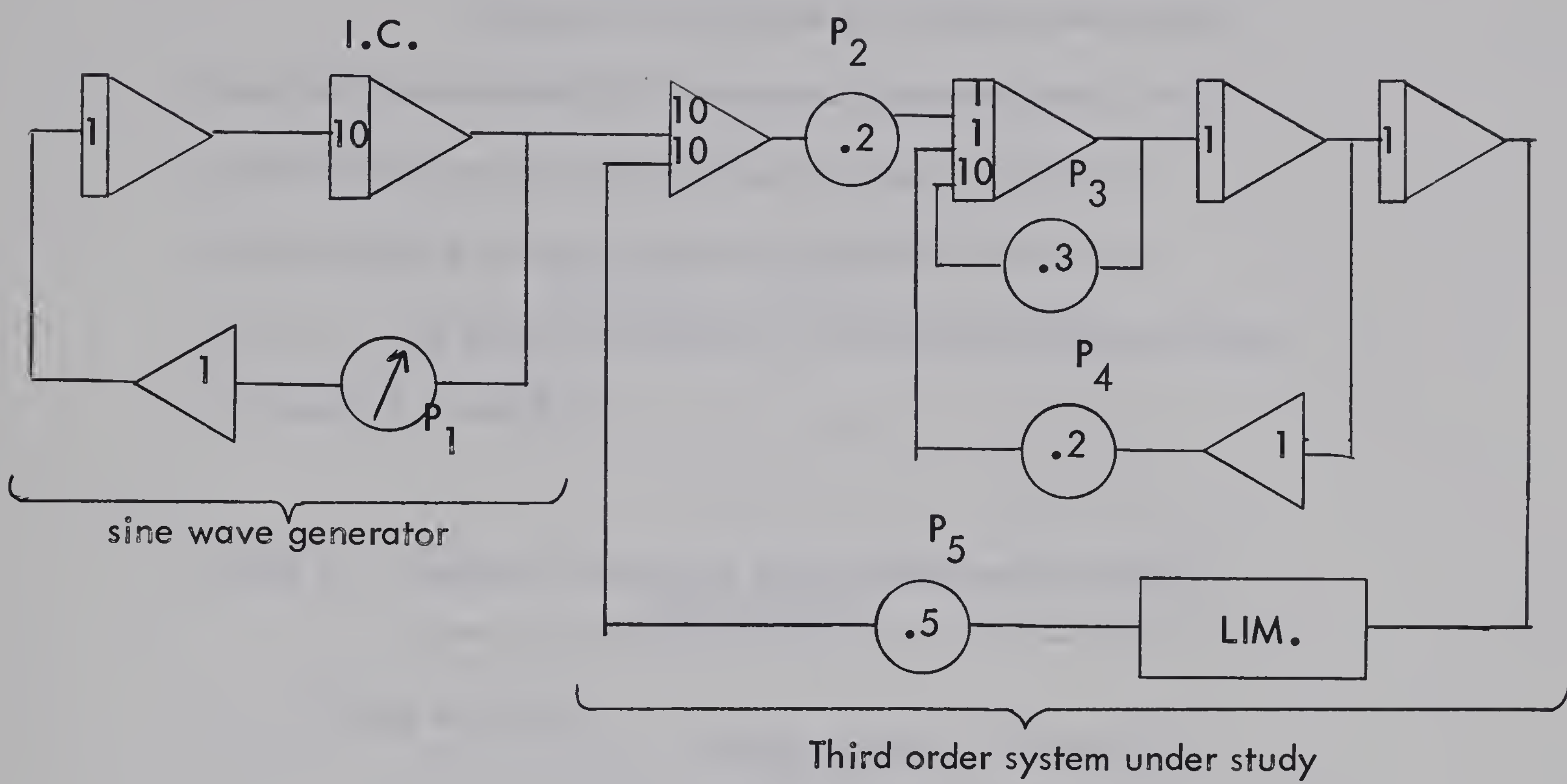

Fig. 4.2 Analog simulation for a third order system

4.2 Experimental Procedure

The slope of the limiter is set to a specific value. The frequency of the input signal is kept constant at a predetermined value. The amplitude of the input signal is varied and the amplitude of the output signal is recorded. All measurements are made under steady state conditions.

Two values of slope of the limiter S = 3 and S = 5 are used and the tests are conducted for second and third order systems.

4.3 Experimental Results

Figures 4.3, 4.4A and 4.4B show the results obtained experimentally for the second order system. The experimental and predicted values of input amplitude at jump resonance for this case are compared in Tables 4.1 and 4.2. The actual waveforms of the system output are shown in Figures 4.5 and 4.6.

Table 4.1 Frequency range for jump resonance for second order system

Slope of limiter S	Experimental	Predicted
3	$0.2 \leq \omega \leq 3.0$	$0.24 \leq \omega \leq 2.2$
5	$0.2 \leq \omega \leq 5.5$	$0.15 \leq \omega \leq 2.9$

Table 4.2 Input amplitude at jump resonance for second order system

Slope of limiter S	Frequency of input signal (rad/sec)	Input amplitude at jump resonance Experimental	Predicted
3	0.5	3.2	3.32
3	1.0	2.8	2.82
3	1.5	2.5	2.13
5	0.5	5.75	5.7
5	1.0	5.10	5.18
5	1.5	4.7	4.24
5	2.0	4.45	3.38*

* The predicted value at $\omega = 2$ is not too reliable as this frequency corresponds to a point on the $G(\omega)$ curve very close to the X-axis, thus rendering the semigraphical construction difficult and inaccurate.

4.3 Experimental Results (cont'd)

Similarly the results for the third order system are shown in Figures 4.7 and 4.8 and Tables 4.3 and 4.4

Table 4.3 Frequency range for jump resonance for a third order system

Slope of limiter S	Experimental	Predicted
3	$.23 \leqslant \omega \leqslant 1.4$	$.25 \leqslant \omega \leqslant 1.5$
5	$.125 \leqslant \omega \leqslant 1.7$	$.12 \leqslant \omega \leqslant 1.7$

Table 4.4 Input amplitude at jump resonance for a third order system

Slope of limiter S	Frequency of input signal (rad/sec)	Input amplitude at jump resonance Experimental	Predicted
3	0.4	2.8	2.96
3	1.0	1.50	1.59
5	0.4	5.0	5.3
5	0.5	4.1	4.7
5	1.0	2.3	3.2 **

** Footnote * applies also to this case at $\omega = 1$.

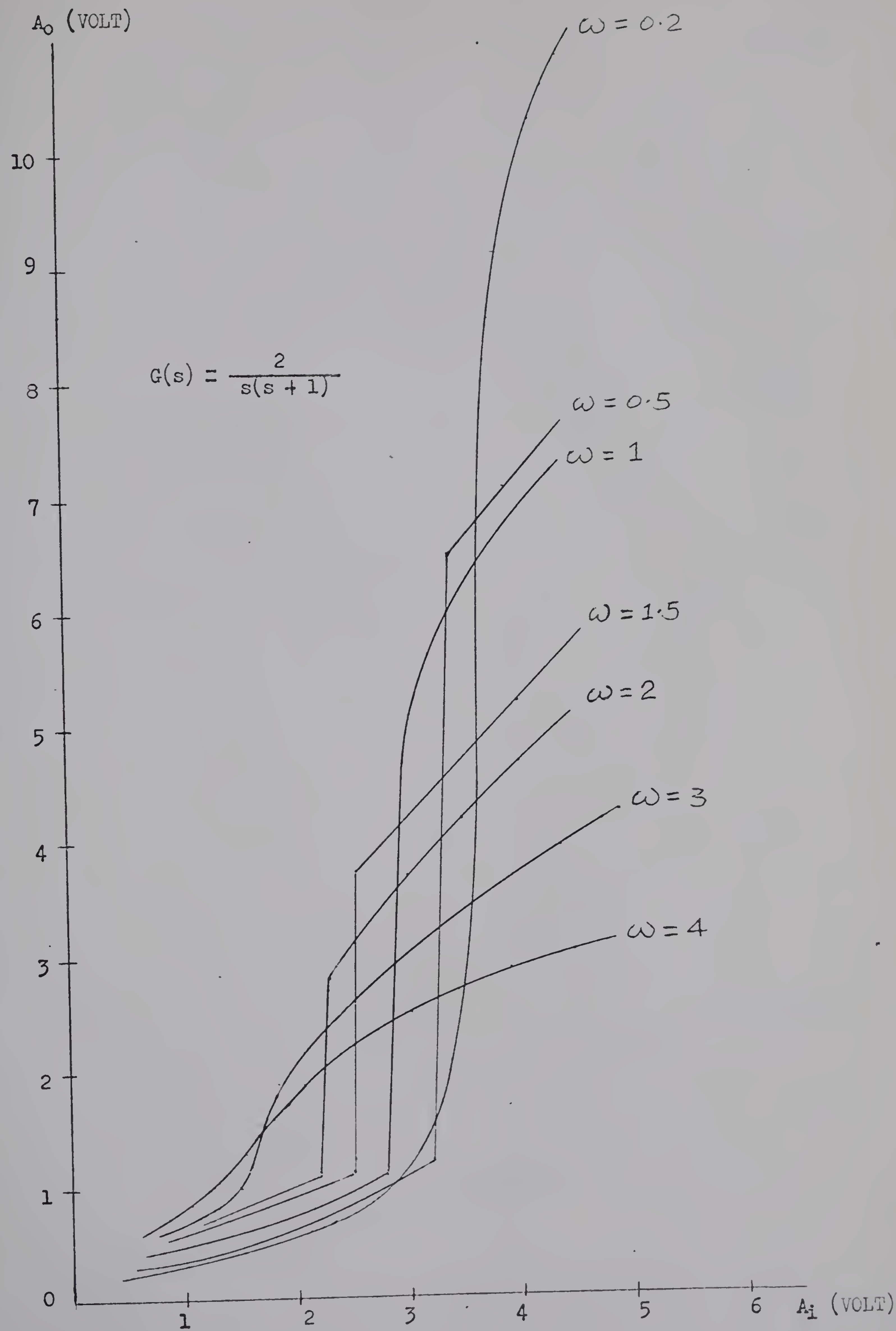

Fig. 4.3 Input-output curves for second order system. S = 3

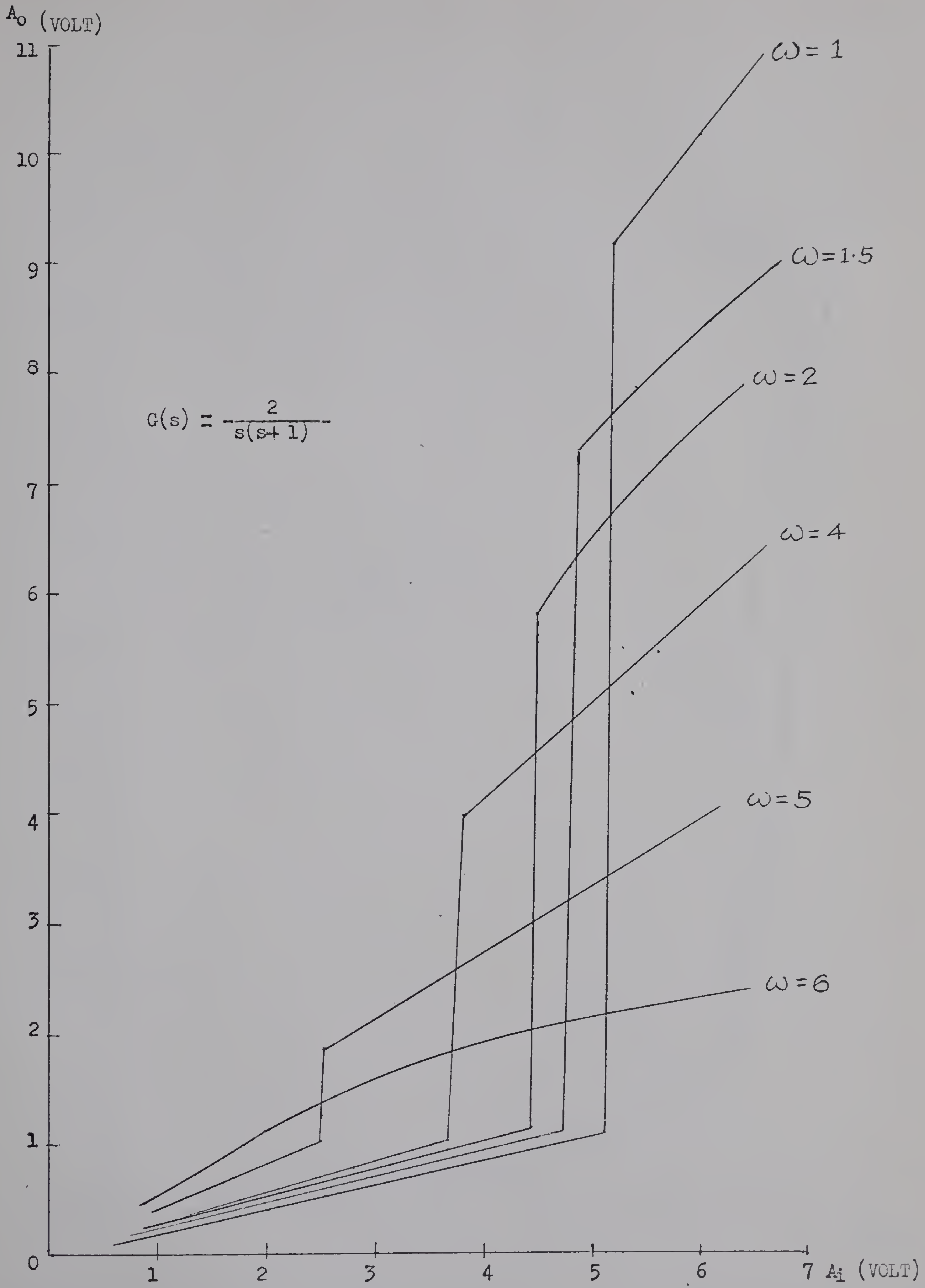

Fig. 4.4A Input-output curves for second order system. S = 5
Frequency range $1 \leq \omega \leq 6$

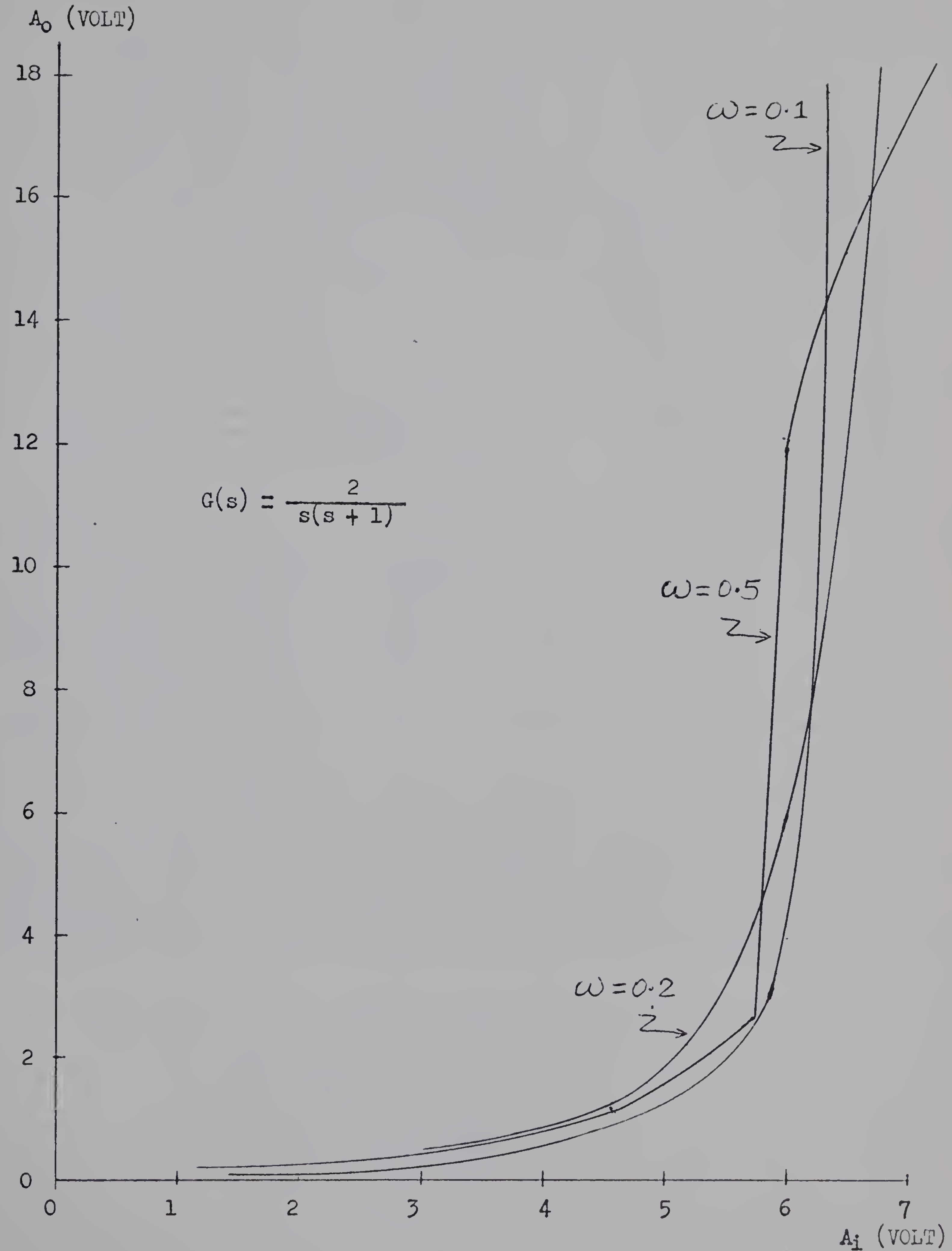

Fig. 4.4B Input-output curves for second order system. S = 5
Frequency range $0.1 \leq \omega \leq 0.5$

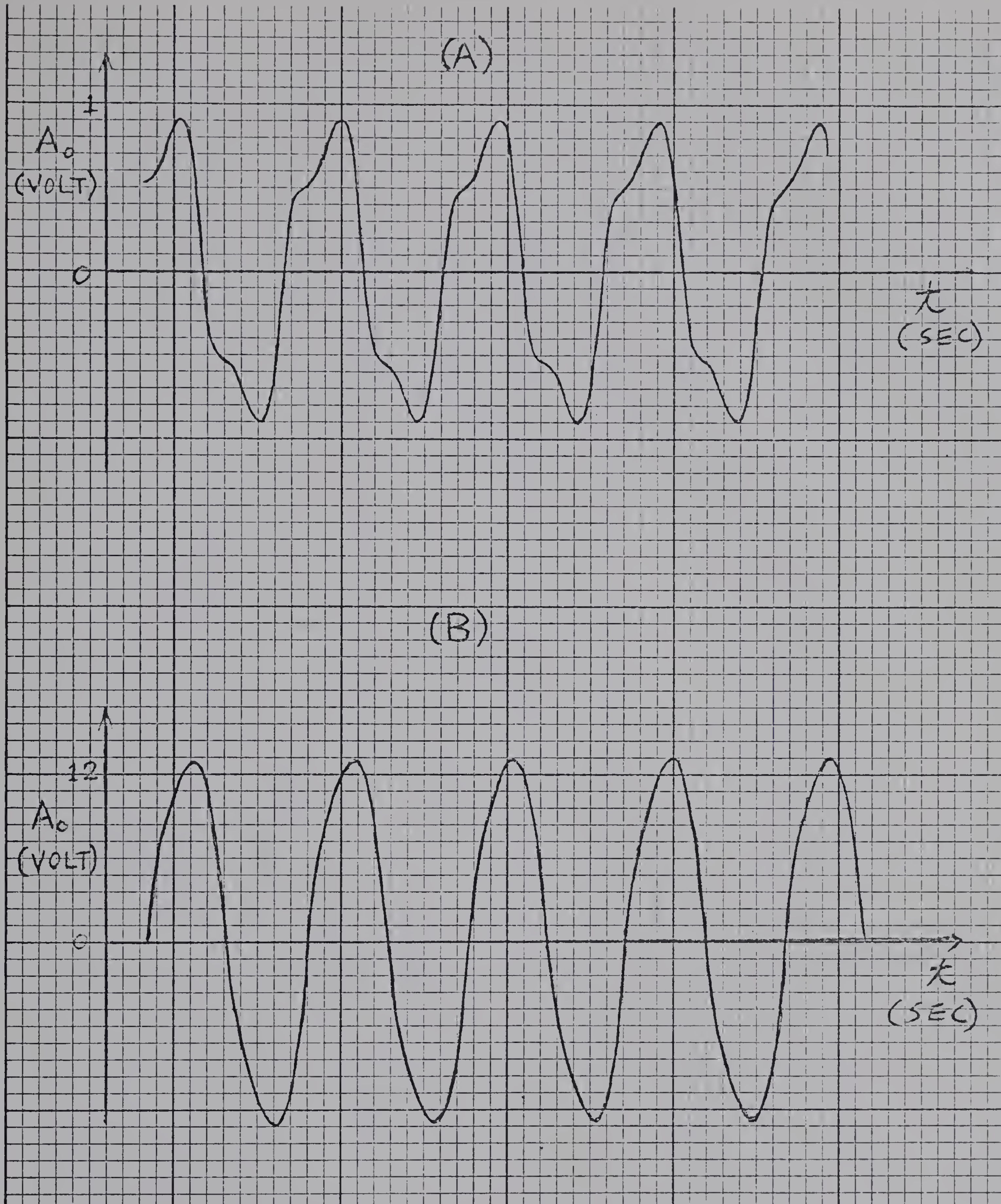

Fig. 4.5. Output waveform for the second order system

$$G(s) = \frac{2}{s(s+1)} \quad \text{at } \omega = 0.5,\ S = 5$$

when (A) $A_i = 4.5$, (B) $A_i = 6$

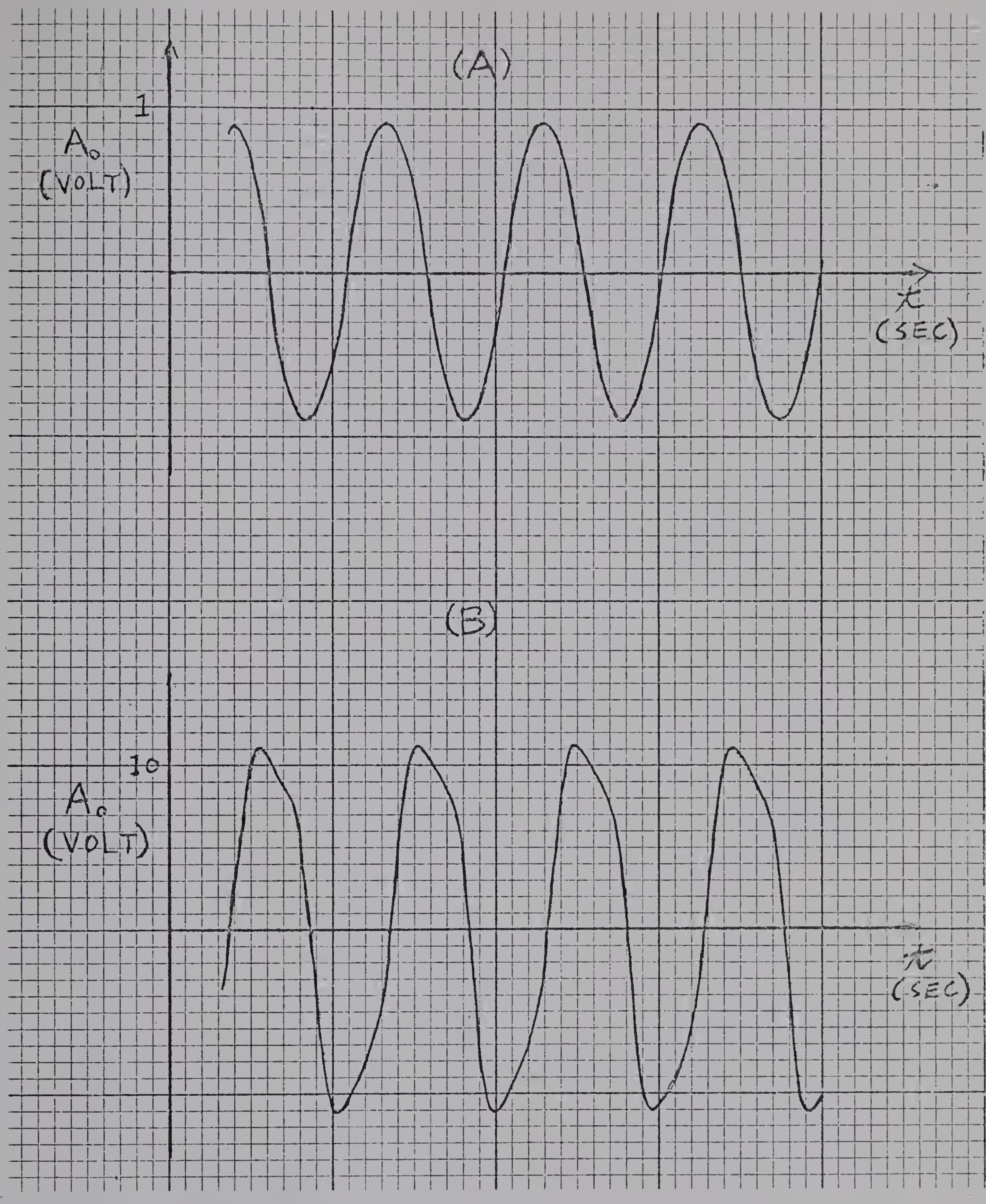

Fig. 4.6 Output waveform for the second order system

$$G(s) = \frac{2}{s(s+1)} \quad \text{at } \omega = 1, \; S = 5$$

when (A) $A_i = 4$, (B) $A_i = 6$

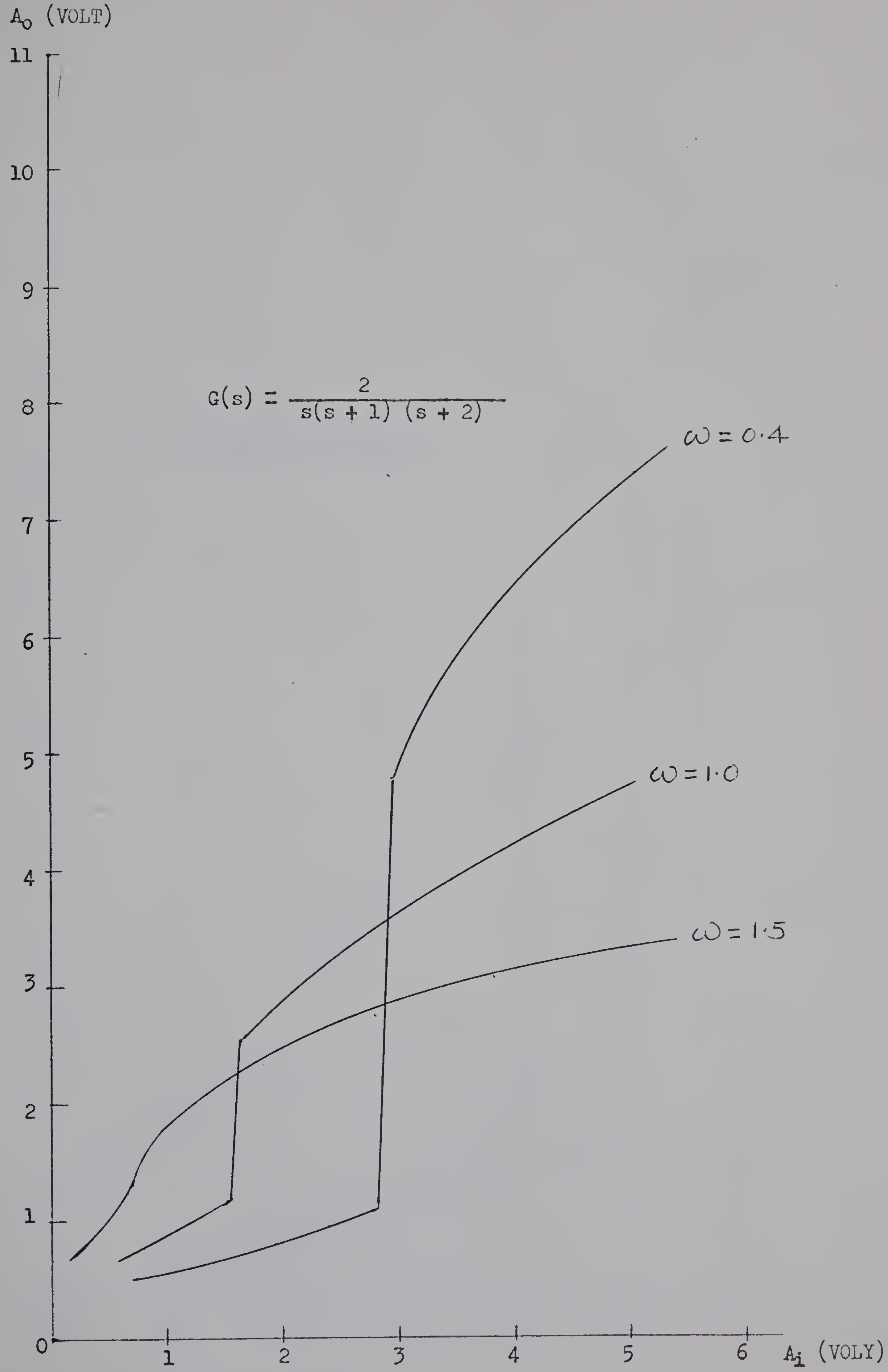

Fig. 4. Input-output curves for third order system. S = 3

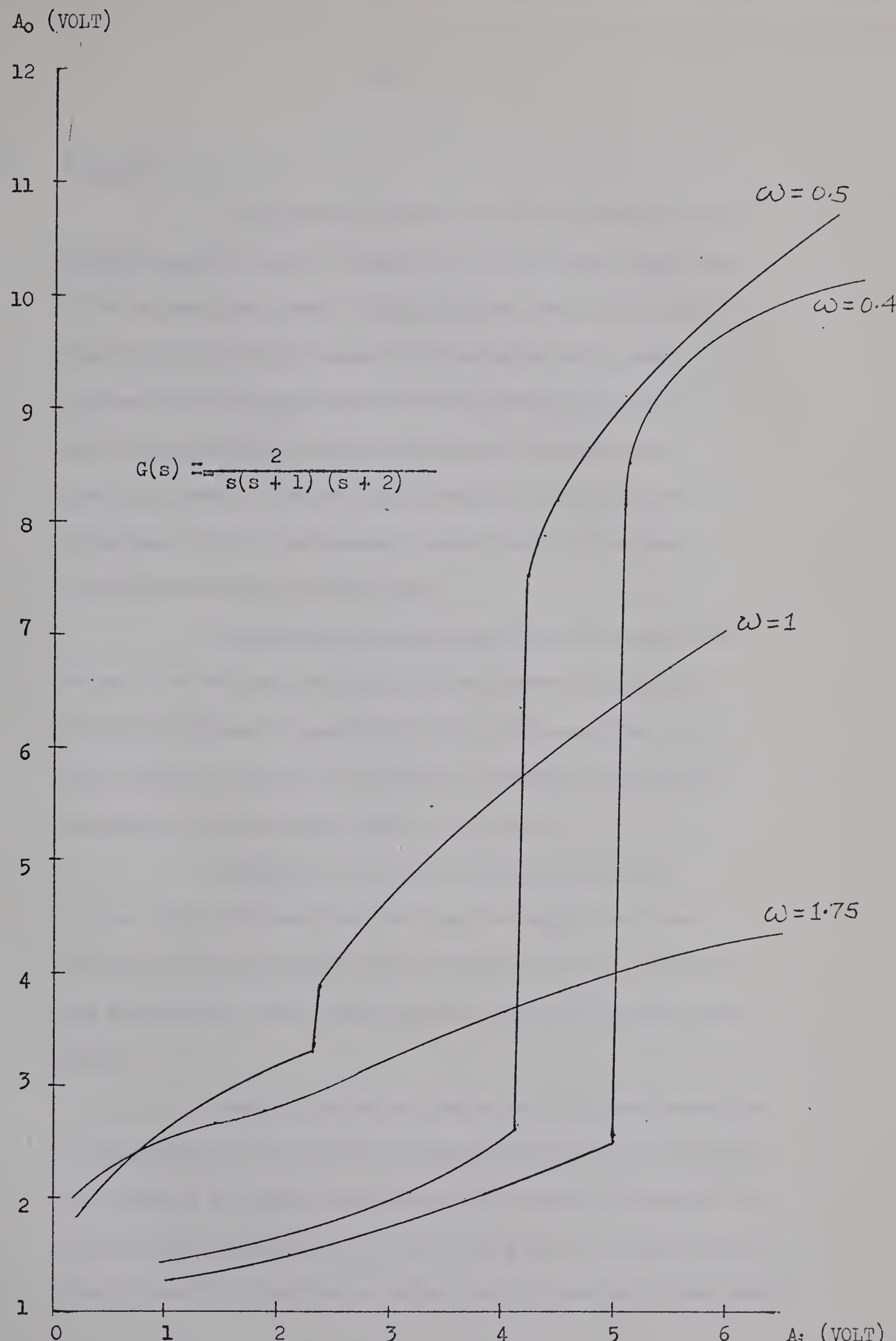

Fig. 4.7 Input-output curves for third order system. S = 5

4.4 Comments

The agreement between experimental and predicted values is generally good; it is better for the third order system than for the second order system. Table 4.2 shows that, with regard to imput amplitude at jump resonance in the second order system, agreement between experimental and predicted values is very good at low frequencies, but the discrepancy increases as frequency increases. A rather large discrepancy is also observed at the upper limit of the frequency range (Table 4.1) for jump resonance in the second order system.

The discrepancy between predicted and experimental values of the frequency range for the jump resonance is found to occur at all values of slope of the limiter which were tried. It is felt, therefore, that there is no apparent correlation between this discrepancy and the value of slope of the limiter.

Changing the location of poles of the transfer function G(s) to different positions along the negative axis does not seem to have any effect on the discrepancy between predicted and experimental values of the frequency range and the input amplitudes.

Based on the above observations, it appears reasonable to state that the most probable explanation for the discrepancies found in the case of the second order system is the imperfect filtering of high frequencies by the plant G. The third order plant, on the other hand, offers a more effective filtering action, and thus provides a better result.

CHAPTER FIVE

COMPENSATION ON JUMP RESONANCE

5.1 Introduction

In control system design, the performance of a closed loop system must be set to meet the given specifications. One possible design procedure is to develop first a model system satisfying the general overall requirements, and then take into account the detailed refinements that should be incorporated into this fundamental model system so that all the given requirements are met. This design procedure employs the commonly used technique of compensation.

In this chapter we shall examine the advantages, if any, of using feedback compensation (derivative type) in order to eliminate the jumps which would otherwise occur. Elimination of jump resonance will make the behaviour of the overall system more predictable.

5.2 Possible Methods of Eliminating Jump Resonance

Looking at the curves in Figures 3.6 and 3.7, it is apparent that jumps can be avoided by shifting the G and EN curves in such a way that they no longer intersect with each other. This can be achieved by the relocation of either

(a) the G curve, or
(b) the EN curve, or
(c) both G and EN curves

5.2 Possible Methods of Eliminating Jump Resonance (cont'd)

We immediately recognize that (b) is impractical because the variables associated with the nonlinearity N are in almost all cases fixed or specified. In other words, it is unlikely, for example, that the slope of the limiter in a real system can be changed. Further, we may have no control over the point where saturation level of the limiter occurs. Case (c) is eliminated for the same reasons. We shall then explore further the remaining possibility, namely, relocation of the $G(\omega)$ locus.

5.3 Effect of Varying K, the Gain of the Linear Plant G(s)

In a number of cases it will be possible to vary K in G(s) where G(s) is of the form

$$G(s) = K \frac{A(s)}{B(s)} \tag{5.1}$$

Varying K will change the size of the $G(\omega)$ locus in the X-Y plane but not its shape. If K is increased, the magnification factor M increases but at the same time the phase shift decreases and vice versa.

One way of eliminating jumps is to decrease K to a sufficiently small value so that the G locus and EN curve do not intersect. But this has the disadvantage that the forward gain will be reduced to a rather small value before the aim is achieved. For the second order system, for example,

$$G(s) = \frac{K}{s(s+1)} \tag{5.2}$$

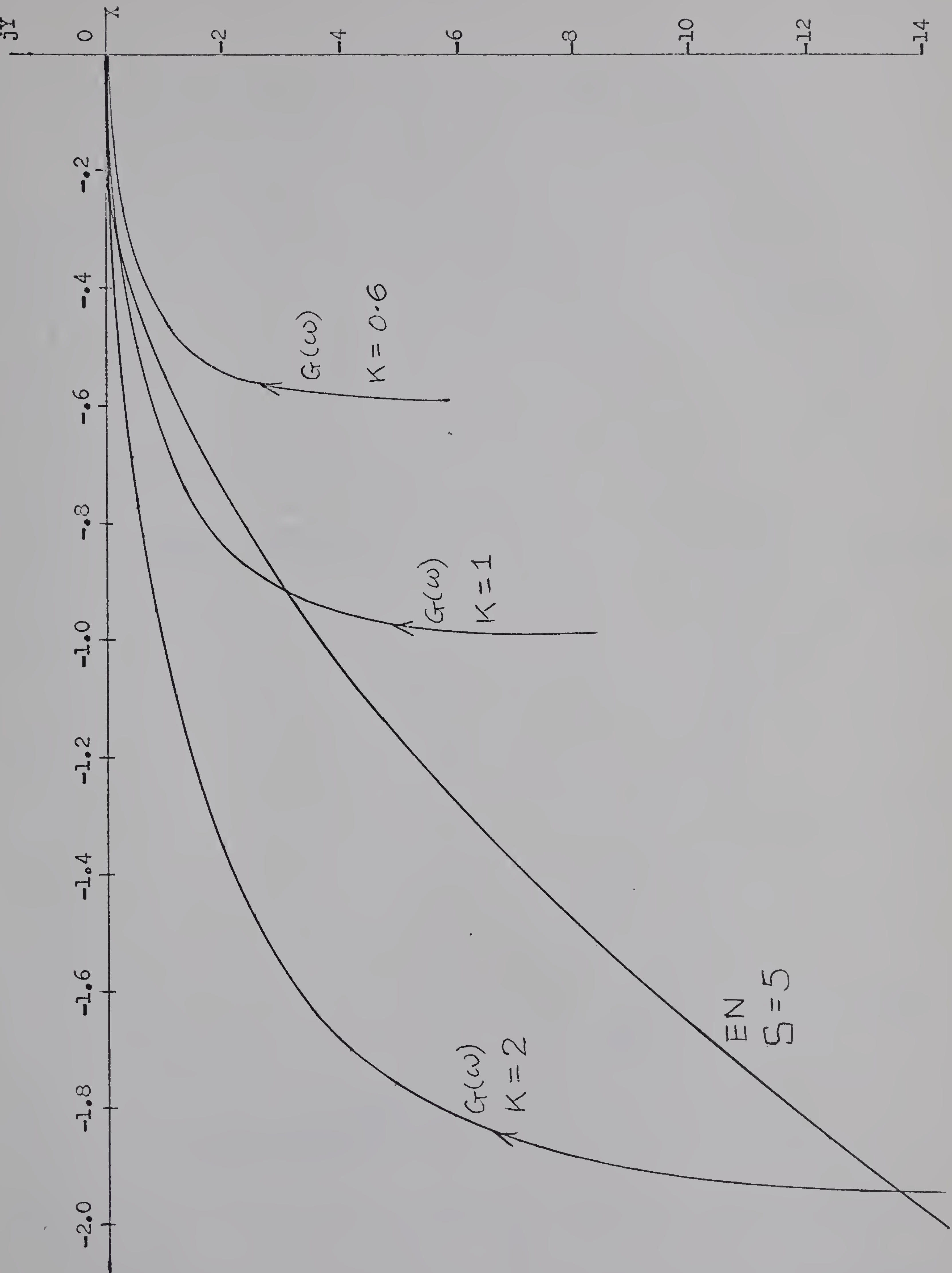

Fig. 5.1 Location of G curves for different values of K

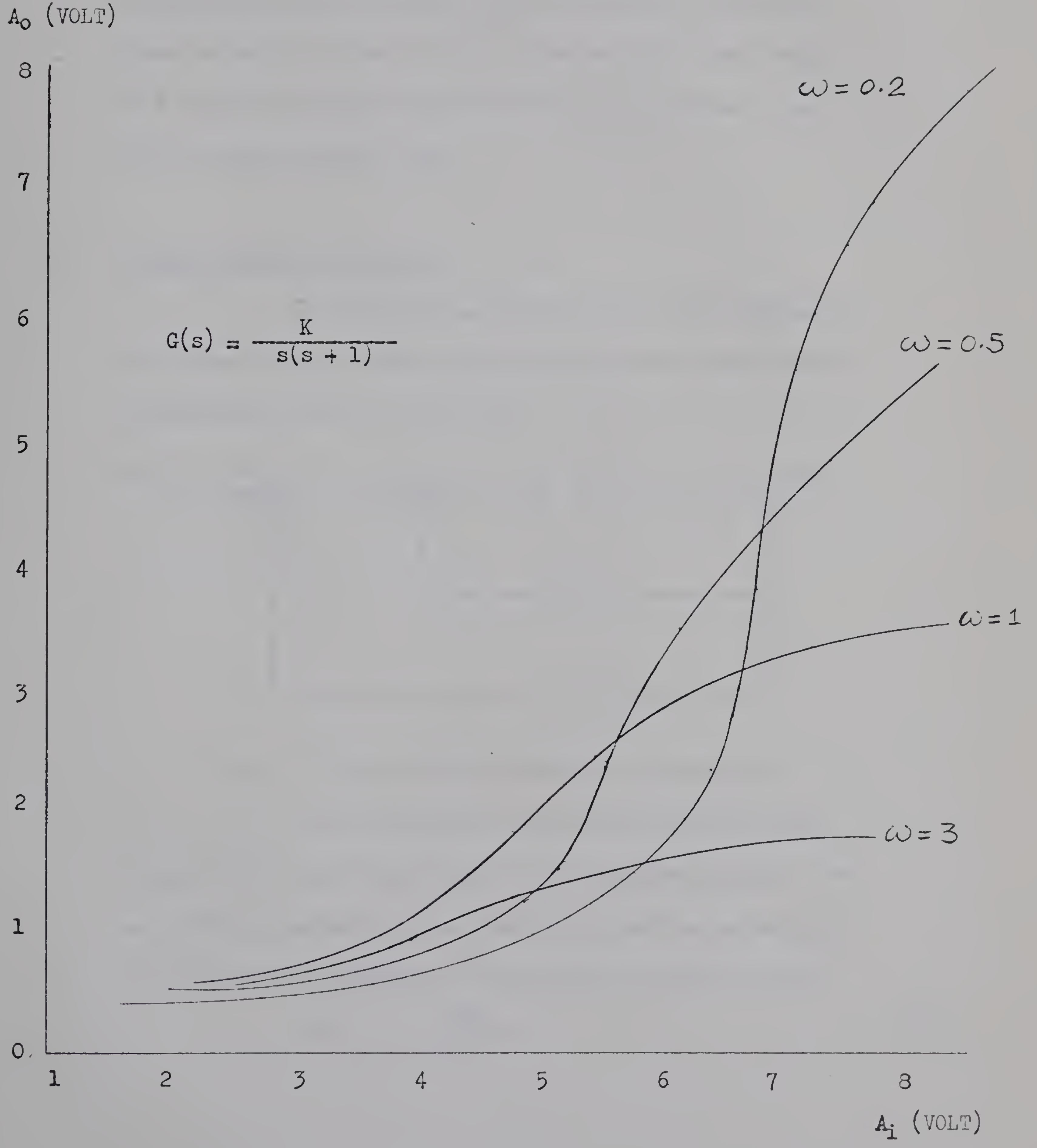

Fig. 5. Input-output curves for second order system. K = 0.6

5.3 Effect of Varying K, the Gain of the Linear Plant G(s) (cont'd)

K will have to be reduced to 0.6 before jumps can be eliminated. This is shown in Fig. 5.1, and is confirmed experimentally. The experimental results are shown in Fig. 5.2 where it is clear that jumps do not occur when K = 0.6. However, such a small value of K may not meet system specifications such as rise time, overshoot, steady state error, etc.

5.4 Output Derivative Feedback

In this section we shall examine another approach to eliminate jumps, namely, the use of output-derivative feedback compensation as shown in Fig. 5.3.

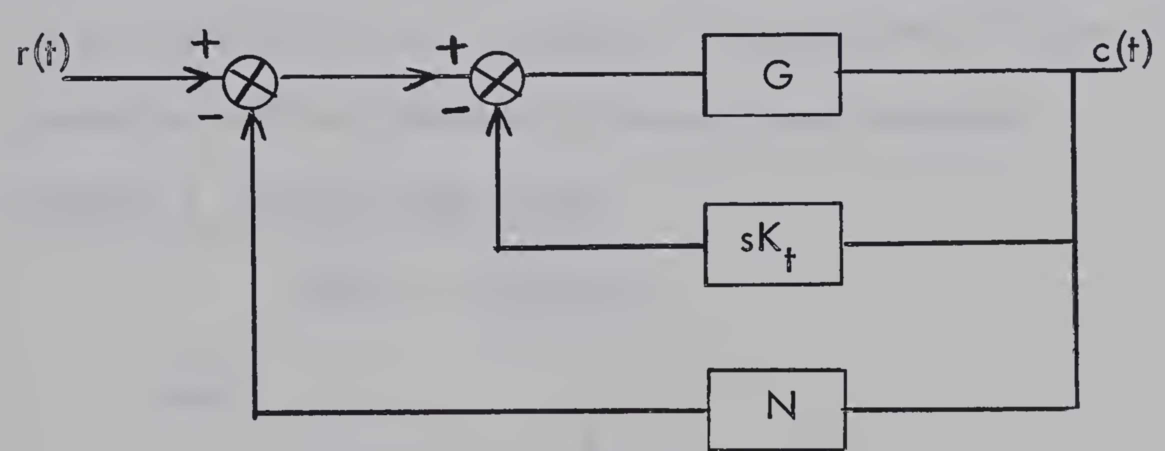

Fig. 5.3 Output-derivative feedback compensation

The forward gain K of the linear plant G is held constant while the feedback factor K_t is considered variable. The effect of this feedback can be taken into account by replacing G by G' where G', the effective linear plant, is related to G by

$$G'(s) = \frac{G(s)}{1 + K_t s} \tag{5.3}$$

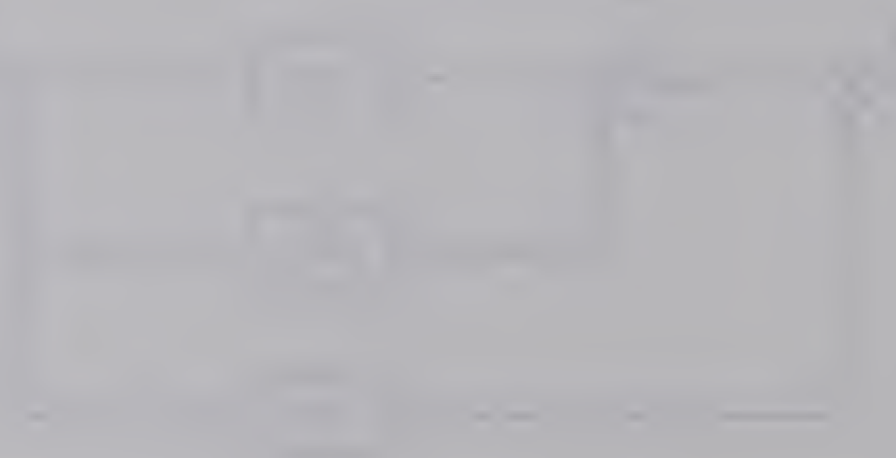

5.4 Output Derivative Feedback (cont'd)

The overall system is now shown in Fig. 5.4

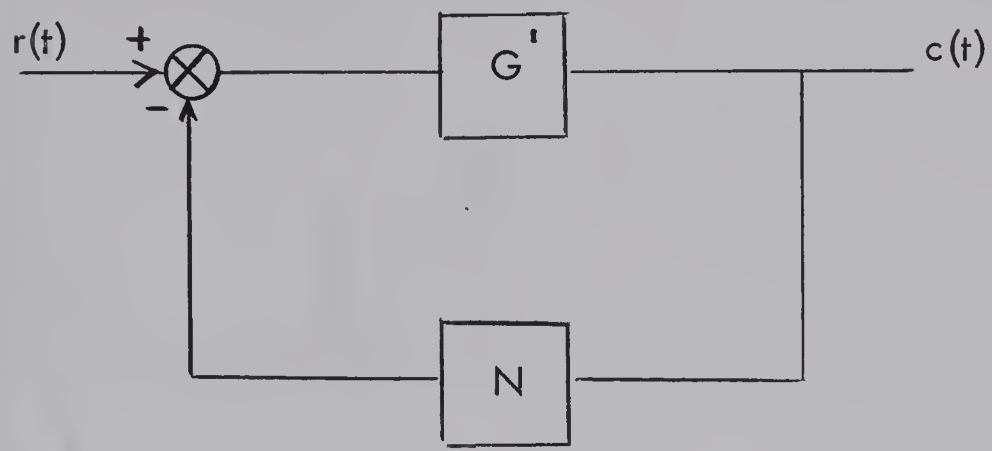

Fig. 5.4 The equivalent system

The semigraphical procedure described in Chapter Two can now be applied to the system in Fig. 5.4. The G' locus is plotted for different value of K_t and superimposed on the EN curve. K_t is varied till the G' locus does not intersect the EN curve. This procedure will be illustrated by means of two examples.

Example 1 - Second order system

$$G(s) = \frac{2}{s(s+1)} \tag{5.4}$$

and

$$G'(s) = \frac{2}{s^2 + s(1 + 2K_t)} \tag{5.5}$$

The G' locus for $K_t = 0.5$ and the EN curve for $S = 5$ are shown in Fig. 5.5. This system is simulated on the computer and the effect of K_t on the jump resonance is investigated. These results are shown in Fig. 5.6. It is clear that the jumps are eliminated.

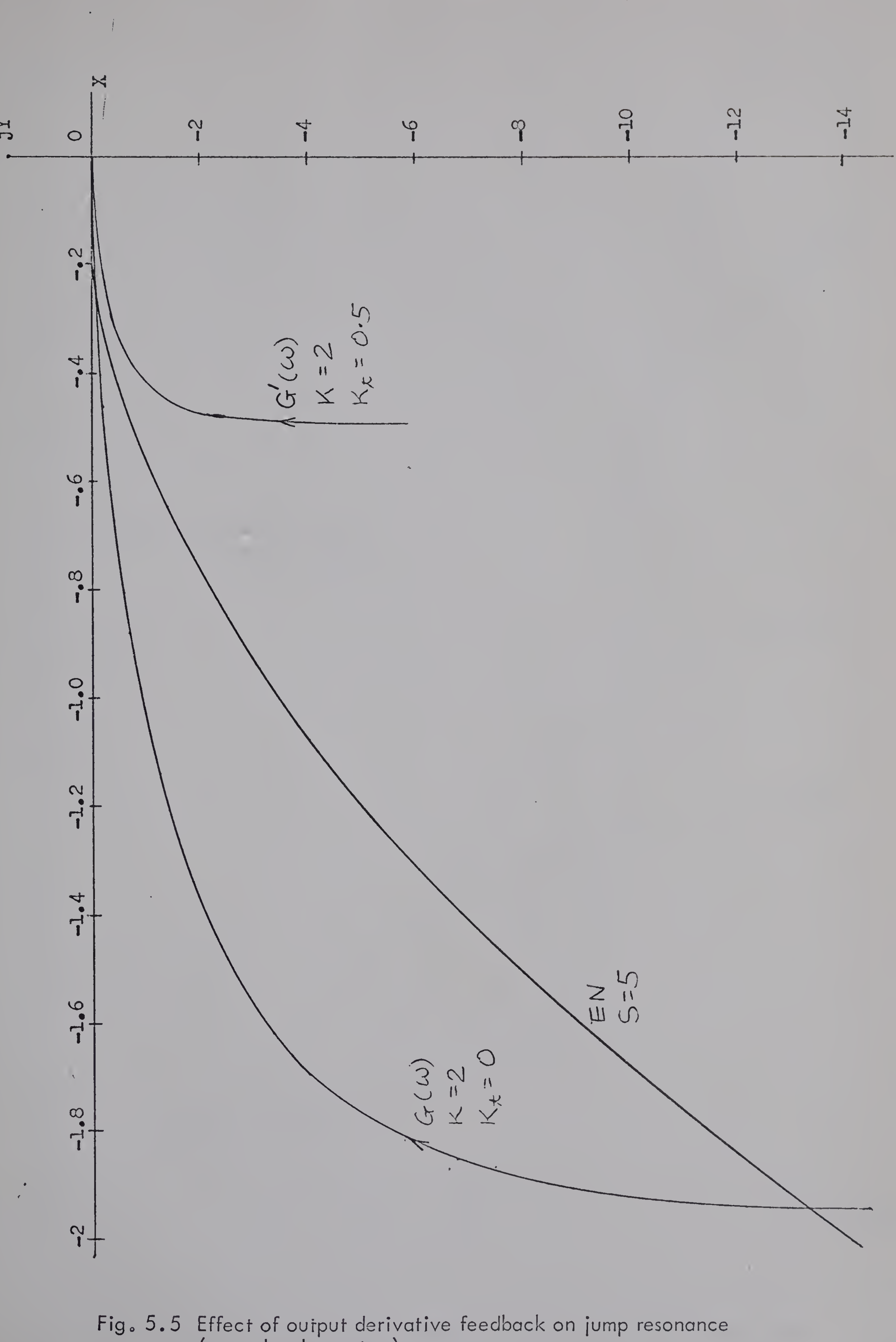

Fig. 5.5 Effect of output derivative feedback on jump resonance
(second order system)

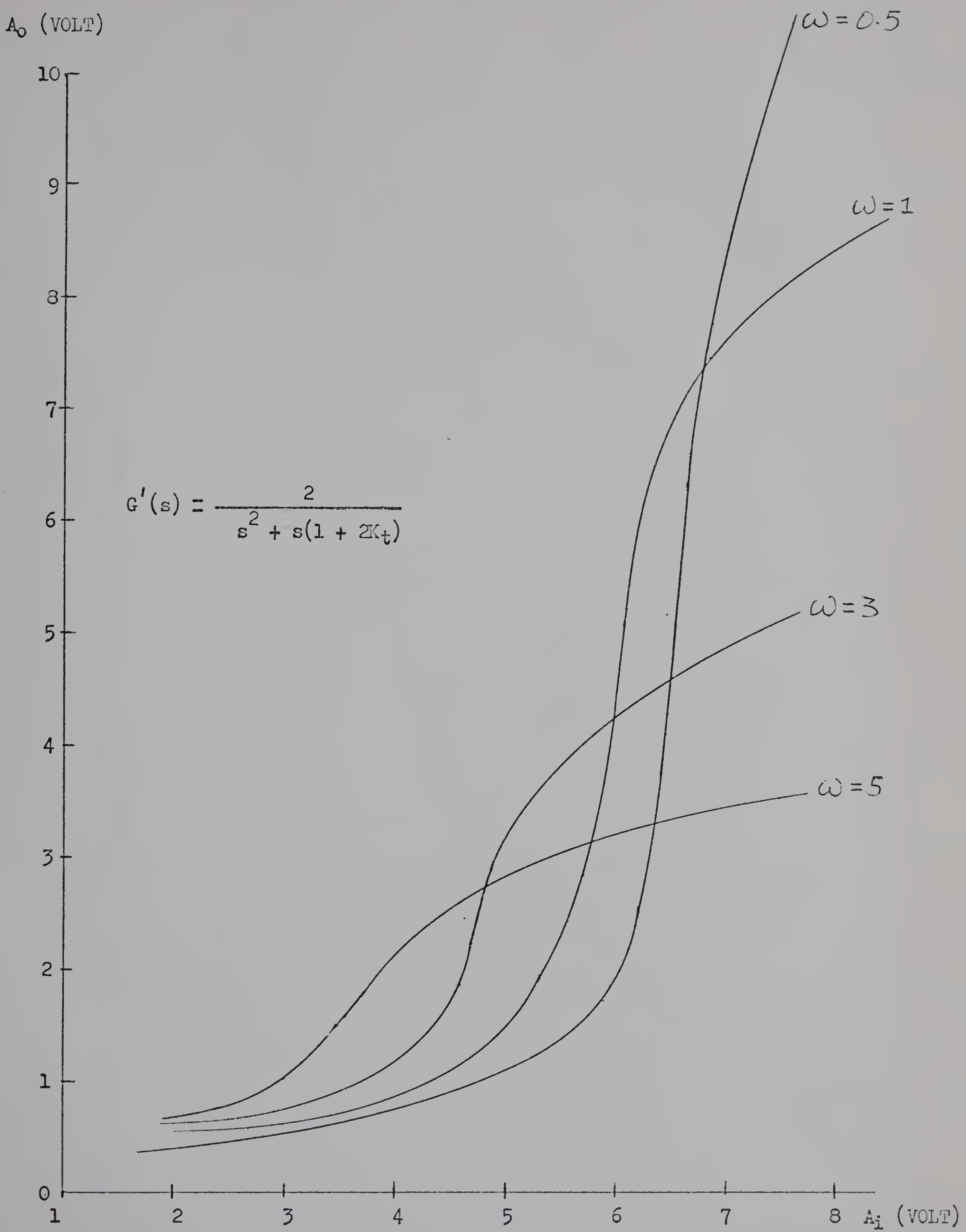

Fig. 5.6 Input-output curves for compensated second order system

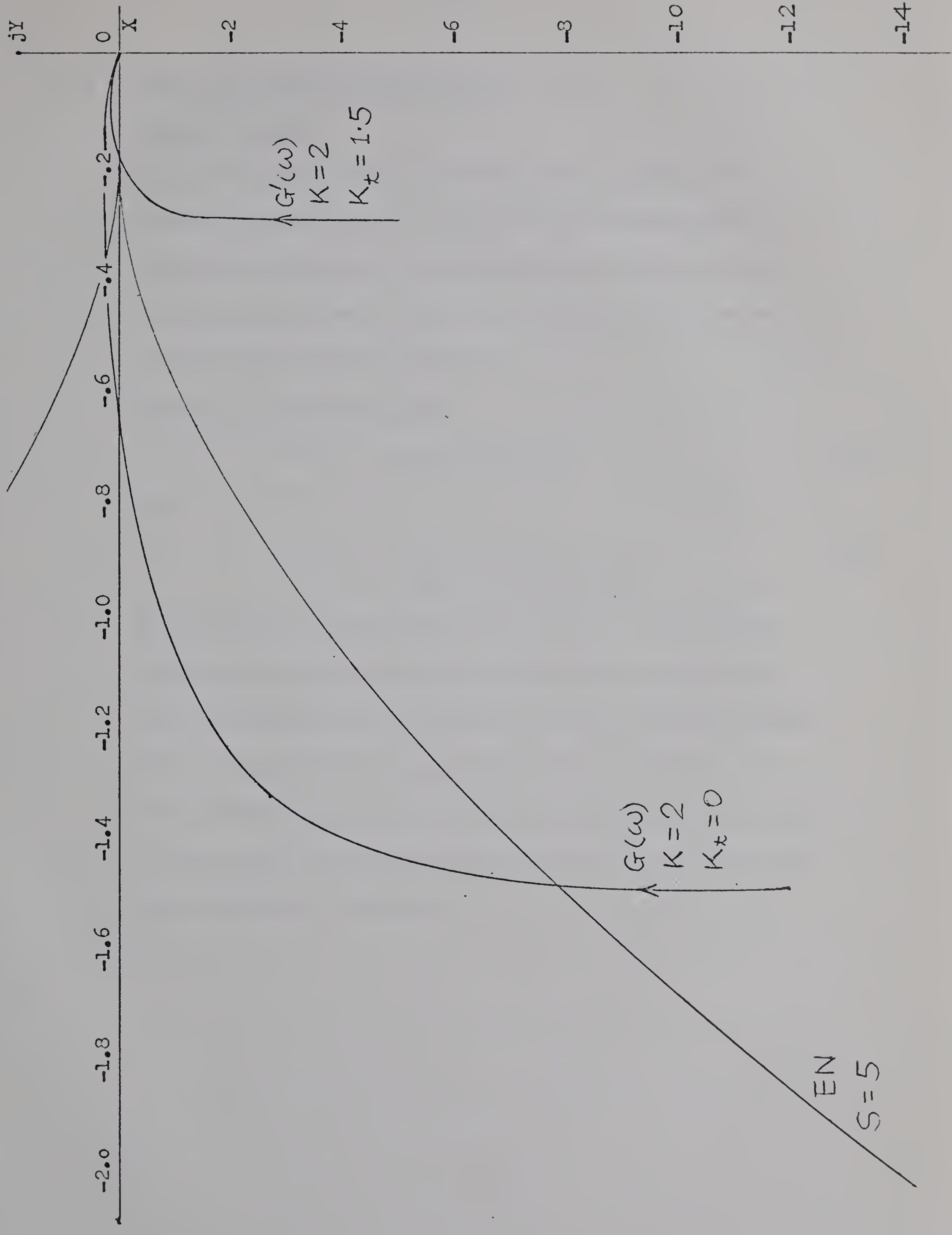

Fig. 5.7 Relocation of G curves by introducing compensation (third order system)

5.4 Output Derivative Feedback (cont'd)

Example 1 (cont'd)

It is worth mentioning that by increasing the value of K_t, G' moves further away from EN in Fig. 5.5. This indicates further improvement in the overall system performance as far as avoiding the jumps are concerned. Thus, a value of $K_t \cong 0.5$ will insure a smooth system response in this case.

Example 2 - Third order system

$$G(s) = \frac{2}{s(s+1)(s+2)} \tag{5.6}$$

and

$$G'(s) = \frac{2}{s\left[s^2 + 3s + (2 + 2K_t)\right]} \tag{5.7}$$

The G and EN curves are shown in Fig. 5.7. It is clear that the G curve must be relocated in such a position that the intersections in both the second and third quadrants of the X-Y plane are avoided. This is accomplished by choosing values of K_t such that $K_t \cong 1.5$. It is confirmed experimentally that the input-output curves are smooth as in the case of the compensated second order system. These curves hence will not be included here.

SUMMARY AND CONCLUSION

A method has been presented to investigate the phenomenon of jump resonance in the class of nonlinear systems with a single-valued nonlinear element in the feedback loop. The Describing Function of the nonlinear element is assumed to be frequency independent. The work presented here should complement Hatanaka's work which is suitable for analyzing similar phenomenon in the class of systems in which the same type of nonlinear element is in the forward loop. The location of the saturation type nonlinearity will no longer, as it has done so far, cause any difficulties.

It appears that the method presented in this thesis is more suitable to systems of third order or higher. When it is applied to a second order system, greater caution should be exercised, particularly in determining the upper limit of the frequency range for jump resonance. The reasons for this limitation have been explained in the thesis.

It also seems possible that similar procedures could be developed for systems with multi-valued and/or frequency dependent nonlinearities. Work along this line is difficult but challenging enough to warrant further investigation.

BIBLIOGRAPHY

1. Hayashi, C., "Forced Oscillations in Nonlinear Systems", Nippon Printing and Publishing Co. Ltd., Osaka, Japan, 1953.

2. Ogata, K., "An Analytic Method for Finding the Closed Loop Frequency Response of Nonlinear Feedback Control Systems", Trans. AIEE, Vol. 76 (1957), Pt. 11, pp. 277-285.

3. Lewis, J.B., "The Use of Nonlinear Feedback to Improve the Transient Response of a Servomechanism", Trans. AIEE, Pt. 11, Vol. 71 (1952), pp. 447-453.

4. West, J.C., J.L. Douce and Livesley, R.K., "The DIDF and Its Use in the Analysis of Nonlinear Feedback Systems", Proc. IEE, Vol. 103 (1956), B, pp. 463-474.

5. Prince, L. Jr., "A Generalized Method for Determining the Closed-Loop Frequency Response of Nonlinear System", Trans. AIEE, Vol. 73, Pt. 11 (1954), pp. 217-224.

6. Levinson, E., "Some Saturation Phenomena in Servomechanism with Emphasis on the Tachometer Stabilized Systems", Trans. AIEE, Pt. 11, Vol. 72 (1953), pp. 1-9.

7. Hatanaka, H., "The Frequency Responses and Jump Resonance Phenomenon of Nonlinear Feedback Control Systems", Trans. ASME, Basic Eng. Series D, 1963, pp.236-242.

8. Sridhar, R., "A General Method for Deriving the Describing Functions for a Certain Class of Nonlinearities", IRE trans. on A.C. Vol. 5, pp. 135-141, 1960.

9. Gibson, J., "Nonlinear Automatic Control", McGraw-Hill, New York, 1963.

10. Osgood, W.A., "Advanced Calculus", Macmillan Company, N.Y. 1952, pp. 186-187.

11. Jackson, A., "Analog Computation",McGraw-Hill, New York, 1960.

APPENDIX "A"

SUMMARY OF SOME MAIN RESULTS BY HATANAKA

Referring to Fig. 1.1, we get

$$r(t) = A_i \sin \omega t$$

$$e(t) = E \sin (\omega t + \alpha) \qquad (A.1)$$

$$c(t) = A_o \sin (\omega t + \phi)$$

and $G(\omega) = X(\omega) + jY(\omega)$

It can be shown that the output-input amplitude ratio M is given by

$$M = \frac{R}{E} = N(E) \sqrt{\left\{X(\omega) + [N(E)]^{-1}\right\}^2 + \left\{Y(\omega)\right\}^2} \qquad (A.2)$$

and the jump resonance point is

$$\left\{X + [N(E)]^{-1}\right\}\left\{X + [N(E) + E N'(E)]^{-1}\right\} + Y^2 = 0 \qquad (A.3)$$

The expression for the critical jump resonance curve is given by the equation (A.4) with E as a parameter.

$$X = - \frac{N'(E)\, N^*(E) + N(E)\, N^{*\prime}(E)}{N'(E) \left\{N^*(E)\right\}^2 + N^{*\prime}(E)\left\{N(E)\right\}^2}$$

$$Y = \pm \frac{\sqrt{N'(E)\, N^{*\prime}(E)}\, \left\{N(E) - N^*(E)\right\}}{N'(E) \left\{N^*(E)\right\}^2 + N^{*\prime}(E) \left\{N(E)\right\}^2} \qquad (A.4)$$

where

$$N^*(E) = N(E) + E N'(E)$$

APPENDIX "B"

Referring to Fig. 2.5, slope of tangent to the point P on the curve $G(\omega)$ is given by

$$m_i = \left(\frac{\partial y}{\partial x}\right)_i \tag{B.1}$$

Equation of a line perpendicular to the tangent line whose slope is m_i will have a slope of $-\frac{1}{m_i}$ and the equation of this line is

$$Y = -\frac{1}{m_i} X + B \tag{B.2}$$

where B is a constant.

At ω_i, $X = X_i$, $Y = Y_i$

$$\text{then } B = Y_i + \frac{1}{m_i} X_i \tag{B.3}$$

Substituting into (B.2), we get

$$Y = -\frac{1}{m_i} X + Y_i + \frac{1}{m_i} X_i \tag{B.4}$$

APPENDIX "C"

DERIVATION OF DESCRIBING FUNCTION FOR THE LIMITER

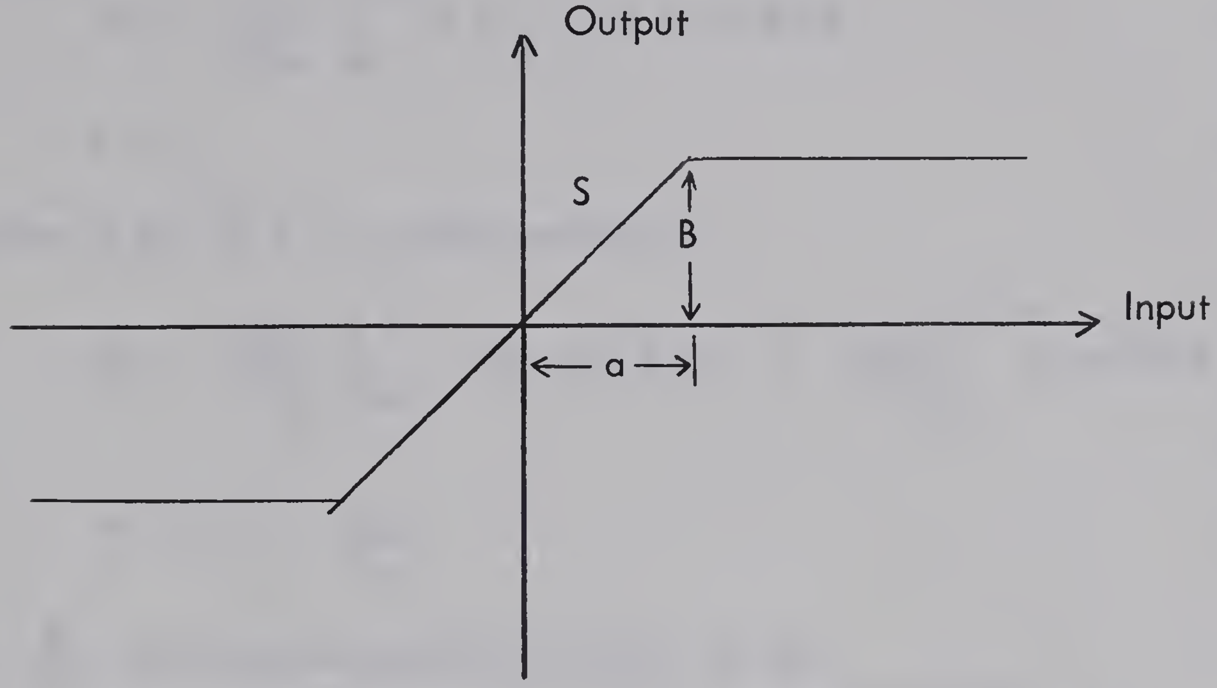

Fig. C. A limiter representation

For a linear element, transfer function defines a unique input-output relationship. In the case of a nonlinear element, the Describing Function relates output to input only in some sense. Usually the describing function of a nonlinear element is defined as the ratio of the amplitude of the fundamental component obtained by Fourier analysis of the output to the amplitude of the sinusoidal input (ref. 11), that is,

$$N = \frac{\text{amplitude of output fundamental component}}{\text{amplitude of sinusoidal input}} \tag{C.1}$$

Let input to the limiter be

$$R = A_o \sin \omega t \tag{C.2}$$

Appendix "C" (cont'd)

Then

$$N = \frac{1}{\pi A_o} \int_0^{2\pi} f(A_o \sin\theta) \sin\theta \, d\theta \tag{C.3}$$

where $\theta = \omega t$ (C.4)

For the limiter in Fig. B.1, it is easily seen that

$$N = \frac{2}{\pi A_o} \int_{-\theta}^{o} S A_o \sin^2\theta \, d\theta + \frac{2}{\pi A_o} \int_{o}^{\pi-\theta} B \sin\theta \, d\theta \tag{C.5}$$

where $\theta = \sin^{-1} \frac{a}{A_o}$ (C.6)

Using $S = \frac{B}{a}$ and substituting for S in (C.5), we get

$$N = \frac{2B}{\pi a} \left[\sin^{-1}\left(\frac{a}{A_o}\right) + \left(\frac{a}{A_o}\right) \frac{\sqrt{A_o^2 - a^2}}{A_o} \right] \tag{C.7}$$